THE NEW KEYNESIAN CLIMATE MODEL

JEAN-GUILLAUME SAHUC FRANK SMETS GAUTHIER VERMANDEL

ABSTRACT. Climate change confronts economies with two inflationary challenges: *climateflation*, driven by physical climate impacts, and *greenflation*, arising from mitigation efforts. This paper develops and estimates a nonlinear New Keynesian Climate model that merges the long-term dynamics of Integrated Assessment Models with the business cycle fluctuations captured by DSGE frameworks. This unified framework enables a systematic analysis of how climate change and mitigation policies influence inflation, output, and interest rates. We find that nominal rigidities are crucial for determining optimal carbon pricing: neglecting them leads to miscalibrated carbon taxes, excessive inflation, and reduced consumption. Simulations also reveal that Paris-aligned mitigation paths generate higher inflation than laissez-faire approaches. Nonetheless, central banks can counter these inflationary pressures by adapting policy to a rising natural interest rate and accepting short-term GDP losses. These results highlight the need to align monetary frameworks with climate policy goals to ensure macroeconomic stability during the net-zero transition.

JEL: E32, E52, Q50, Q54.

Keywords: Climate change, inflation, monetary policy, environmental New-Keynesian model, environmental and economic trends, Bayesian estimation

J.-G. Sahuc: Banque de France, 31 rue Croix des Petits Champs, 75049 Paris, France, and University Paris-Nanterre (e-mail: jean-guillaume.sahuc@banque-france.fr). F. Smets: Bank for International Settlements, Centralbahnplatz 2, 4051 Basel, Switzerland, Ghent University and CEPR (frank.smets@ugent.be). G. Vermandel: CMAP, Ecole Polytechnique, Institut Polytechnique de Paris, Route de Saclay, Palaiseau, University Paris-Dauphine & PSL, LEDA UMR CNRS 8007, Place du Maréchal de Lattre de Tassigny, 75016 Paris, France, and Banque de France (e-mail: gauthier@vermandel.fr). We thank Nicoletta Batini, Ghassane Benmir, Marco Del Negro, Simon Dietz, Francesca Diluiso, Stephie Fried, Lars Peter Hansen, John Hassler, Fanny Henriet, Felix Kluber, Noémie Lisack, Anton Nakov, Conny Olovsson, Maria Sole Pagliari, Evi Pappa, Philipp Pfeiffer, Ricardo Reis, Fabien Tripier, Rick van der Ploeg as well as participants in several workshops and conferences for helpful comments The views expressed in this paper are those of the authors and do not necessarily reflect the views of the Banque de France, the Eurosystem, or the Bank for International Settlements. Declarations of interest: none.

1. Introduction

Conventional Integrated Assessment Models (IAMs), including those employed by the Intergovernmental Panel on Climate Change to evaluate specifically the long-term transition to a low-carbon economy, are formulated entirely in real terms and abstract from the nominal dimensions of climate change and climate policy.[1] Yet, two inflationary forces, *climateflation*, stemming from climate-related disruptions to productivity, and *greenflation*, arising from transition policies such as carbon taxes and abatement spending, are increasingly shaping both the macroeconomic consequences and the political feasibility of the net-zero transition. The New-Keynesian (NK) framework, which explicitly models nominal rigidities and the transmission of monetary policy, offers a natural foundation for incorporating these nominal effects. However, standard New-Keynesian models are designed for short- to medium-term analysis and omit the long-term structural transformations central to climate dynamics. This disconnect underscores the need for a unified framework that captures the long-term dynamics of climate change and the nominal frictions essential to monetary policy.

This paper presents the New Keynesian Climate (NKC) model, a tractable, nonlinear framework for the global economy that bridges the gap between Integrated Assessment Models and New Keynesian models. This new framework is deliberately designed to preserve the analytical clarity and tractability of traditional macroeconomic models, such as those developed by Woodford (2003) and Galí (2008), while incorporating key features to capture climate externalities and abatement costs. In addition, it captures the first-order real and nominal effects of the green transition and enables a systematic analysis of the evolving role of central banks in managing its macroeconomic consequences amid long-term structural shifts.

The NKC consists of four core equations: the IS curve, which incorporates green investment to reduce carbon emissions; the Phillips curve, which accounts for the economic damage from rising carbon stocks and the production costs of abatement efforts; the monetary policy rule, which links the nominal interest rate to inflation deviations from target and the output gap; and a law of motion governing the accumulation of carbon dioxide emissions, which is influenced by current production levels and abatement efforts. Importantly, the model incorporates five exogenous trends (population, carbon intensity, abatement efficiency, the inflation target, and technological progress) to account for observed structural changes over the long run. These trends are essential in macro-climate models as they enable accurate forecasts of future carbon emissions and hence climate change. Neglecting these structural trends may result in inaccurate quantitative predictions, especially concerning future climate

[1] Fernández-Villaverde et al. (2025) provide a comprehensive review of recent advances in structural IAMs, focusing on the integration of natural science with general equilibrium macroeconomic frameworks and computational methods.

change, which can shape expectations and, in turn, bias even current policy recommendations. Focusing on a tractable global economy framework is a natural starting point before turning to more disaggregated analysis, but also offers three main advantages: *(i)* it enables a clear analytical decomposition of inflationary effects; *(ii)* it allows for direct comparison with existing IAMs, many of which are formulated at the global level; and *(iii)* it sidesteps the complexity of modeling emissions trajectories across multiple economies. While monetary frameworks vary across countries, most central banks operate under inflation-targeting regimes and respond to shared structural forces, resulting in a strong co-movement of policy rates. In particular, the usual targets are highly correlated due to factors such as synchronized business cycles (Rey, 2015) and the globalization of supply chains, which has contributed to the emergence of a global Phillips curve (Auer et al., 2017). In this context, the NKC model offers a tractable yet reasonable representation of the aggregate interactions between climate policy and monetary policy in the face of rising temperatures or coordinated carbon taxation.

A central contribution of this paper is the full-information estimation of the NKC model using novel methods tailored to its intrinsically nonlinear structure. Whereas traditional IAMs often rely on calibration, limiting empirical validation and weakening their policy relevance (Pindyck, 2013), we introduce empirical discipline into a climate-integrated macroeconomic framework, consistent with the standards of modern quantitative macroeconomics. Persistent structural trends make conventional perturbation techniques unsuitable, as local approximations around a deterministic steady state break down. To address this, we simulate and estimate the model using unanticipated shocks (commonly referred to as "MIT shocks") and assume no aggregate uncertainty. Specifically, we develop a new filtering approach that treats the model itself as the data-generating process, enabling direct statistical evaluation against four global macroeconomic and climate-related time series from 1985Q1 to 2023Q2. Finally, our Bayesian framework allows us to quantify parametric uncertainty across climate policy scenarios, complementing existing studies that emphasize uncertainty in emissions pathways (IPCC, 2021), long-run climate-economic risks (Cai and Lontzek, 2019; Van den Bremer and Van der Ploeg, 2021), and structural uncertainty in climate system calibration, which shapes the social planner's problem (Folini et al., 2025).

Armed with this estimated model, we assess the role of price rigidities and monetary policy during the green transition, specifically its response to climateflation and greenflation, across different transition scenarios. The first scenario is a "laissez-faire" economy characterized by an increasing stock of carbon, that warms the planet and makes resources scarcer. The increasing damage to total factor productivity acts as a permanent negative supply shock

that fuels inflation and drives output below its technological trend (Schnabel, 2022). The second scenario reflects the Paris Agreement, under which governments worldwide coordinate mitigation policies aimed at achieving net-zero carbon emissions by 2050. In our framework, this scenario takes the form of a linear increase in the carbon tax such that full abatement is reached in 2050. The rise in carbon tax forces firms to internalize the effects of their carbon emissions on aggregate productivity. In response, they reduce their emissions by increasing abatement expenditures, creating a demand-driven boom. These scenarios serve to *(i)* explore the trade-offs between immediate abatement efforts and future climate-induced damages, and *(ii)* examine their implications for natural output, natural interest rate, inflation dynamics, and the appropriate monetary policy responses.

Our analysis yields five key findings. First, under the estimated monetary policy reaction function, we find that a green transition aligned with the Paris Agreement leads to higher and more persistent inflation compared to a laissez-faire environmental policy. It means that the inflationary effects of greenflation outweigh the disinflationary effects from reduced climate damages (climateflation). This result proves robust across multiple alternative model specifications, including the introduction of wage rigidities and investment adjustment costs. Second, we identify a crucial intertemporal trade-off for central banks: the short-term costs of the green transition, manifested in greater volatility of inflation and output, must be weighed against the long-term gains in output and consumption. Delaying the transition exacerbates the economic consequences of climate damages, with output dispersion increasing by roughly 30% after 2050. Third, our results highlight the inflationary risks of conventional monetary policy rules when they fail to adapt to a rising natural rate. In particular, static Taylor rules based on deviations from a fixed steady-state interest rate overlook the structural upward shift induced by the low-carbon transition, resulting in an average inflation overshoot of 0.7 percentage points per year during the transition period. In contrast, climate-adaptive policy rules that internalize changes in the natural rate more effectively stabilize inflation throughout the transition. Fourth, the social cost of carbon, that is, the optimal price for emitting one ton of CO_2, is lower in an economy with sticky prices than in a flexible-price setting. This reflects a fundamental trade-off between price stability and climate ambition. If inflation is not well-managed during the green transition, the rising welfare cost of inflation weakens the case for aggressive carbon pricing, thereby reducing the optimal social cost of carbon. In effect, when the transition leads to sustained inflation above target, optimal climate policy becomes less ambitious: people place less value on future climate benefits when their current purchasing power is eroded by inflation. This underscores how price instability can undermine long-term environmental goals. Finally, we highlight the macroeconomic

effects of using a miscalibrated carbon price. Most climate-economic models used to guide policy, including those behind official carbon pricing estimates, ignore how inflation affects the economy during a net zero transition. As a result, the carbon prices they recommend may be poorly suited to real-world conditions, where prices adjust slowly. We show that applying such misaligned prices can lead to significant economic costs, including lower household consumption and added inflationary pressure. These challenges are particularly acute during the green transition, when carbon pricing is politically sensitive. To design climate policies that are both effective and publicly acceptable, it's essential to account for how inflation and other nominal factors shape economic responses.

Related Literature. Our paper contributes to the broader literature that integrates climate considerations into micro-founded structural macroeconomic models, continuing the research agenda initiated by Nordhaus (1992) and extended in Barrage and Nordhaus (2024). This literature spans multiple dimensions, including the distributional consequences of climate adaptation (Fried, 2022), the heterogeneous effects of energy and carbon price shocks (Benmir and Roman, 2022; Auclert et al., 2023; Känzig, 2023), optimal fiscal policy responses to climate change (Barrage, 2020), the role of market structure (Finkelstein Shapiro and Metcalf, 2023; Jondeau et al., 2023), comparative evaluations of environmental policy instruments (Annicchiarico and Di Dio, 2015) and the influence of uncertainty on carbon pricing strategies (Jensen and Traeger, 2014; Cai and Lontzek, 2019; van der Ploeg and Rezai, 2020; Van den Bremer and Van der Ploeg, 2021).[2] Our paper also contributes to an emerging strand of research, often referred to as the greenflation literature, which quantitatively examines the inflationary consequences of the green transition. Recent studies have investigated how climate policy interacts with monetary policy in nonlinear macroeconomic settings. For instance, Nakov and Thomas (2023), using a nonlinear New Keynesian model with climate externalities, analyze how optimal monetary policy navigates the trade-off between price stability and climate goals, with the response hinging on the optimality of climate policy itself. Other work shows that the inflationary effects of the green transition depend critically on monetary policy design and production structure. Similarly, Olovsson and Vestin (2023) and Del Negro et al. (2023) use multi-sector models with nominal rigidities to explore how sectoral substitution influences the inflationary effects of the green transition. Targeting core inflation helps contain volatility from energy price spikes, while production network complementarities amplify input cost shocks, intensifying inflation. In a small open economy setting, Pappa et al. (2023) highlight the importance of energy efficiency and the need for complementary fiscal

[2] A related strand of literature examines how the direction of technological change and shifts in the energy mix influence the cost and feasibility of the transition. While this work is important for understanding long-run structural adjustments, it is less directly connected to our focus on nominal frictions and inflation dynamics.

measures to facilitate a smoother transition. Finally, Fornaro et al. (2025) show that capping dirty goods production raises inflation and steepens the Phillips curve, complicating central banks' efforts to balance inflation and output.

Our approach departs from the existing literature in several important respects, offering a distinct contribution to the analysis of the nominal consequences of climate change. First, we contribute to the greenflation literature by developing a deliberately simple framework that isolates the core inflationary mechanisms triggered by both climate policy and climate damages. While much of the literature focuses narrowly on greenflation, we extend the analysis to include climateflation. Crucially, we decompose these forces prior to general equilibrium adjustments, providing transparent accounting of their respective contributions. Although both channels are quantitatively significant ex ante, their inflationary impact may be attenuated by general equilibrium forces, particularly through wage responses. Second, unlike most existing work that relies on calibrated models, we estimate a nonlinear structural framework. This grounds our analysis in the empirical methodology of modern quantitative macroeconomics, following the tradition of Smets and Wouters (2007). As a result, our simulations are not merely illustrative: they are generated from a fully estimated model and constitute true out-of-sample forecasts. This estimation approach disciplines both the model's parameters and its initial conditions, ensuring internal consistency over the dynamic transition path. Third, our framework allows for full transition paths to net-zero emissions, in line with scenarios assessed by the IPCC. Much of the existing literature relies on constant elasticity of substitution (CES) production functions that reduce emissions through substitution between "brown" and "green" inputs. While analytically convenient, this formulation tends to inhibit full decarbonization, as it implies sharply increasing relative prices as emissions approach zero. It also assumes fixed substitutability across time, despite growing empirical evidence that this elasticity may evolve Jo and Miftakhova (2024). By contrast, we adopt empirically validated abatement cost curves from the DICE model (Barrage and Nordhaus, 2024), which reflect evidence synthesized in recent IPCC reports. This allows us to study a wide range of transition scenarios, ranging from continued warming to full decarbonization, within a tractable, data-driven macro-environmental framework.

The remainder of this paper is organized as follows. Section 2 presents the micro-foundations of the NKC and its summary into four core equations. Section 3 presents the data transformation, and prior and posterior distributions. Section 4 presents the anatomy of the green transition and analyzes how climateflation and greenflation phenomena may affect the world economy by 2100. Section 5 discusses the implications of the green transition for the central

bank. Section 6 examines the concept of social cost of carbon within our framework. Section 7 presents additional exercises to check the robustness of the analysis. Section 8 concludes.

2. The 4 equation New Keynesian climate (NKC) model

To establish a flexible framework conducive to analytical results, we incorporate climate dynamics, drawing on the integrated assessment framework of Nordhaus (1992) and the damage-cost approach of Golosov et al. (2014), into the standard three-equation New Keynesian model, as developed in Woodford (2003) and Galí (2008).

2.1. Household sector.

The economy consist of a time-varying mass l_t of ex-ante identical, atomistic, and infinitely lived households. This mass reflects the upward trend in population observed over the past 60 years, with l_t asymptotically converging to a long-run level $l_\infty > 0$, according to the process: $l_t = l_{t-1}\left(l_\infty / l_{t-1}\right)^{\ell_g}$, where $\ell_g \in [0,1]$ is the geometric rate of convergence to l_∞. Each household $i \in [0, l_t]$ maximizes its utility over time, which depends positively on consumption $c_{i,t}$ and negatively on labor $n_{i,t}$:

$$\mathbb{E}_t \left\{ \sum_{s=0}^{\infty} \tilde{\beta}_{t,t+s} \varepsilon_{b,t+s} \left(\frac{c_{i,t+s}^{1-\sigma_c} - 1}{1-\sigma_c} - \psi_{t+s} \frac{n_{i,t+s}^{1+\sigma_n}}{1+\sigma_n} \right) \right\}, \tag{1}$$

where $\mathbb{E}_t$ denotes the conditional expectation at time t, and $\tilde{\beta}_{t,t+s}$ is the technological-neutral discount factor.[3] The parameter $\sigma_c > 0$ represents the inverse of the intertemporal elasticity of substitution in consumption, while $\sigma_n > 0$ is the inverse of the Frisch labor supply elasticity. ψ_t is a scale variable determining hours worked in a balanced growth path, growing proportionally with the flow of consumption.[4] The preference shock $\varepsilon_{b,t}$, which captures unexpected changes in aggregate demand, follows an AR(1) process: $\varepsilon_{b,t} = (1-\rho_b) + \rho_c \varepsilon_{b,t-1} + \eta_{b,t}$, where $\eta_{b,t} \sim \mathcal{N}(0, \sigma_b^2)$.

As in McKay et al. (2017), households are endowed with stochastic idiosyncratic employment status $\varsigma_{i,t} \in \{0,1\}$, where 0 indicates low productivity (denoted "type L" worker) and 1 indicates high productivity (denoted "type H" worker). Productivity is drawn i.i.d. with probabilities $\Pr(\varsigma_{i,t} = 0) = \omega$ and $\Pr(\varsigma_{i,t} = 1) = 1 - \omega$. The real budget constraints for each

[3] The presence of a permanent increase in technology affects the Euler equation, and consequently the natural real interest rate and the monetary policy rule. To keep the framework tractable, we mute the effect of technology on the long-run equilibrium rate by imposing: $\tilde{\beta}_{t,t+s} = \beta(z_{t+s}/z_t)^{\sigma_c}$ with $\beta \in (0,1)$. This assumption is standard in models featuring recursive utility functions such as Epstein-Zin for instance.

[4] If z_t denotes the trend in per capita consumption, $\psi_t = \psi z_t^{1-\sigma_c}$, with ψ as a scale parameter.

household type are:

$$c_{i,t} + b_{i,t} + T^s_{i,t} = \frac{r_{t-1}}{\pi_t} b_{i,t-1} + \Pi_{i,t} + w_t n_{i,t} + \frac{T^e_{i,t}}{1-\omega}, \text{ if } \varsigma_{i,t} = 1, \tag{2}$$

$$c_{i,t} + b_{i,t} = \frac{r_{t-1}}{\pi_t} b_{i,t-1} + d_{i,t}, \text{ if } \varsigma_{i,t} = 0, \tag{3}$$

where $b_{i,t}$ is the one-period riskless bond, r_t is the gross nominal interest rate, $\pi_t = p_t/p_{t-1}$ is gross inflation with p_t being the price index, $\Pi_{i,t}$ are real dividends from firm shares, w_t is the aggregate real wage, and $T^e_{i,t}$ is the lum-sum carbon tax transfer. Low-productivity households receive $d_{i,t}$ units of the consumption good as a transfer, while high-productivity households pay a tax of $T^s_{i,t} = \omega d_{i,t}/(1-\omega)$ to finance this transfer. The transfer is time-varying, increasing proportionally with productivity z_t and environmental damages (represented by $\Phi(m_t)$, defined subsequently).

The Euler equation for household i with productivity type $q \in \{H, L\}$ is:

$$\varepsilon_{b,t} c^{-\sigma_c}_{i,q,t} \geq \mathbb{E}_t \left\{ \frac{\tilde{\beta}_{t,t+1} \varepsilon_{b,t+1} r_t}{\pi_{t+1}} \left((1-\omega)\, c^{-\sigma_c}_{i,H,t+1} + \omega c^{-\sigma_c}_{i,L,t+1} \right) \right\}, \tag{4}$$

where $c_{i,H,t}$ and $c_{i,L,t}$ represent consumption of high- and low-productivity households, respectively.

2.2. **Business sector.** The business sector is characterized by final good producers who sell a homogeneous final good to households and the government. To produce, they purchase and package differentiated varieties produced by atomistic, infinitely lived intermediate goods firms that operate in a monopolistically competitive market. These intermediate goods firms contribute to climate change by emitting CO_2 as an unintended byproduct of their production process.

2.2.1. *Final good sector.* At every point in time t, a perfectly competitive sector produces a final good Y_t by combining a continuum of intermediate goods $y_{j,t}$, where $j \in [0, l_t]$, according to the technology $y_t = \left[l_t^{-1/\zeta} \int_0^{l_t} {y_{j,t}}^{\frac{\zeta-1}{\zeta}} \mathrm{d}j \right]^{\frac{\zeta}{\zeta-1}}$. The number of intermediate good firms owned by households is equal to the population size l_t. The parameter $\zeta > 1$ measures the substitutability between differentiated intermediate goods. Final good-producing firms take both their output price, p_t, and the prices of intermediate goods, $p_{i,t}$, as given, and beyond their control. Profit maximization leads to the demand curve $y_{j,t} = l_t^{-1} \left(p_{j,t}/p_t \right)^{-\zeta} y_t$, from which we deduce the relationship between the price of the final good and the prices of intermediate goods $p_t \equiv \left[l_t^{-1} \int_0^{l_t} {p_{j,t}}^{1-\zeta} \mathrm{d}j \right]^{\frac{1}{1-\zeta}}$.

2.2.2. *Intermediate goods sector.* An intermediate good j is produced by a monopolistic firm using the following production function:

$$y_{j,t} = \Gamma_t l_t^{1-\alpha} \left(n_{j,t}^d\right)^{\alpha}, \tag{5}$$

where Γ_t represents total factor productivity (TFP), which influences labor demand $n_{j,t}^d$, and $\alpha \in [0,1]$ indicates labor intensity.

The TFP is determined by two components:

$$\Gamma_t = z_t \Phi\left(m_t\right), \tag{6}$$

where z_t is the deterministic component of productivity, and $\Phi(m_t)$ is a damage function that captures the impact of climate change on the production process. The deterministic component follows the process $z_t = z_{t-1}(1 + g_{z,t})$, where $g_{z,t} = g_{z,t-1}\left(1 - \delta_z\right)$ is the productivity growth rate, and δ_z is the rate of decline in productivity. This formulation reflects that productivity growth has slowed over time by a factor δ_z, aligning with the observed deceleration in per capita economic growth over the past century.

Recent advances in climate science, particularly the TCRE (Transient Climate Response to Cumulative Carbon Emissions) framework, have established a robust linear relationship between global temperature increases and cumulative CO_2 emissions (Dietz et al., 2021). To maintain tractability while accurately capturing the climate damages central to our analysis, we adopt this cumulative emissions approach. Specifically, we model climate change through the stock of CO_2, which evolves according to:

$$m_t = m_{t-1} + \xi_m e_t, \tag{7}$$

where e_t denotes anthropogenic CO_2 emissions at time t, and $\xi_m \geq 0$ is a conversion factor from CO_2 to carbon. Climate damages are then specified as an exponential function of cumulative emissions, following Golosov et al. (2014):

$$\Phi(m_t) = \exp\left(-\gamma m_t\right), \tag{8}$$

where γ determines the sensitivity of damages to the carbon stock. This formulation closely approximates the damage functions commonly used in standard DICE models, but expresses damages directly as a function of cumulative carbon emissions rather than temperature.[5]

A firm's CO_2 emissions resulting from its production process are denoted by $e_{i,t}$. These emissions are subject to a carbon tax $\tau_{e,t}$, which aims to internalize the social cost of carbon

[5] An alternative approach would model temperature as directly proportional to cumulative emissions, $\mathcal{T}_t = \xi_T m_t$, and compute damages using a quadratic damage function. This specification yields equivalent results while requiring an additional equation in the system.

emissions. As a result, the firm is incentivized to reduce its impact by investing in emission abatement technology. The abatement effort of the firm leads to a reduction of $\mu_{i,t}$ (in %) in its CO_2 emissions. The firm's emissions are given by:

$$e_{j,t} = \sigma_t \left(1 - \mu_{j,t}\right) y_{j,t} \varepsilon_{e,t},$$

where σ_t denotes aggregate carbon intensity in the production sector. The law of motion for σ_t is $\sigma_t = \sigma_{t-1}(1 - g_{\sigma,t})$, where $g_{\sigma,t}$ captures changes in the rate of carbon decoupling. These changes follow the process: $g_{\sigma,t} = (1 - \delta_\sigma)\, g_{\sigma,t-1}$, where $\delta_\sigma \in [0, 1]$ is the rate of decline in the decoupling trend, reflecting the observed reduction in the emission-to-GDP ratio over the past 60 years. Additionally, a firm's carbon intensity can be temporarily affected by an aggregate exogenous emissions shock $\varepsilon_{e,t}$, given by: $\varepsilon_{e,t} = (1 - \rho_e) + \rho_e \varepsilon_{e,t-1} + \eta_{e,t}$, where $\eta_{e,t} \sim N(0, \sigma_e^2)$ captures cyclical fluctuations in the emissions-to-output ratio. An increase in $\varepsilon_{e,t}$ leads to a cyclical rise in carbon intensity in the production sector.

In practice, firms have three main options to reduce carbon emissions: (i) substituting carbon-intensive technologies with low-carbon technologies; (ii) investing in energy-saving technologies; or (iii) purchasing carbon sequestration. Much of the recent work on greenflation has primarily focused on substitutions.[6] To capture all three types of abatement actions, we introduce an abatement cost function from Barrage and Nordhaus (2024). Each abatement action links a marginal cost of reduction to a corresponding quantity of carbon abated. As the carbon price increases, a larger proportion of emissions is mitigated. This abatement cost function consolidates all forms of mitigation efforts into a simplified representation within a one-good, one-sector economy. The cost of abatement is given by:

$$\mathcal{C}^a_{j,t} = \theta_{1,t} \mu^{\theta_2}_{j,t} y_{j,t}, \tag{9}$$

where $\theta_{1,t} = (p_b/\theta_2)(1 - \delta_{pb})^{t-t_0}\sigma_t$ is the time-varying level of the abatement cost, $p_b > 0$ is a parameter determining the initial abatement costs, and $0 < \delta_{pb} < 1$ captures technological progress, which lowers the cost of abatement by a factor δ_{pb} each year. The literature on directed technological change typically endogenizes the rate of decline in green technologies, which is encapsulated in $\theta_{1,t}$. Finally, $\theta_2 > 0$ represents the curvature of the abatement cost function, which typically exhibits increasing returns in IAM literature.

[6] For instance, Olovsson and Vestin (2023); Nakov and Thomas (2023) examine the macroeconomic effects of decarbonization by modeling the substitution between two energy sources using a constant elasticity of substitution (CES) framework. Del Negro et al. (2023) extend this approach to a multisector setting using input-output linkages. While these studies provide valuable insights into mitigation via input substitution, they emphasize a single channel. In contrast, our framework, drawing from the DICE model, captures a broader range of CO_2 abatement strategies, including energy efficiency, clean technologies, and behavioral changes, through a more stylized aggregate representation.

Intermediate goods producers solve the typical two-stage problem. In the first stage, with the input price w_t given, firms seek to maximize their one-period profits:

$$\max_{\{y_{j,t},\mu_{j,t}\}} mc_{j,t}y_{j,t} - w_t\left(\frac{y_{j,t}}{\Gamma_t}\right)^{1/\alpha} - \mathcal{C}^a_{j,t} - \tau_{e,t}\sigma_t\left(1-\mu_{j,t}\right)y_{j,t}\varepsilon_{e,t} \tag{10}$$

where $mc_{i,t}$ denotes the real marginal cost of producing one additional unit of output.

In the second stage, firms set their selling prices under the Rotemberg price -setting mechanism. The price adjustment cost under this framework is given by:

$$\mathcal{C}^p_{j,t} = \frac{\kappa}{2}\left(\frac{p_{j,t}}{p_{j,t-1}} - \pi^\star_t\right)^2 \frac{y_t}{l_t} \tag{11}$$

where $\kappa > 0$ is the price stickiness parameter, y_t/l_t is the average market share per firm, and $\pi^\star_t$ is the gross inflation target. Following Ireland (2007), Fève et al., 2010 and Del Negro et al. (2015), this target follows a deterministic process as described by:

$$\pi^\star_t = \delta_{\pi^\star}\pi + (1-\delta_{\pi^\star})\pi^\star_{t-1}, \tag{12}$$

where $\delta_{\pi^\star}$ is the convergence rate reflecting the gradual adjustment of monetary authorities' inflation targets, and π is steady-state gross inflation. This trend mirrors the significant decline in inflation and nominal interest rates observed globally since the 1980s, which we attribute to the gradual adoption of inflation-targeting regimes by central banks, leading to a structural reduction in inflation rates.

In New Keynesian models, announced policies, such as climate policy, often lead to implausibly large effects in present value terms, as seen in the forward guidance puzzle discussed by Del Negro et al. (2023). To mitigate the expectation channel of inflation, an exogenous exit shock is introduced, consistent with empirical evidence on the survival rate of firms over time (OECD, 2017). Following Bilbiie et al. (2012), we assume a "death" shock represented by an idiosyncratic variable $\nu_{j,t} \in \{0,1\}$, where $\nu_{j,t} = 0$ with probability ϑ (death) and $\nu_{j,t} = 1$ with probability $(1-\vartheta)$ (survival). Thus, the probability that a firm survives until period $t+s$ is given by $\mathbb{E}_t[\omega_{j,t+s}] = (1-\vartheta)^s$. Consequently, the firm's optimization problem can be expressed as:

$$\max_{\{p_{j,t}\}} \mathbb{E}_t\left\{\sum_{s=0}^{\infty}\Omega_{t,t+s}\left(y_{j,t+s}\frac{p_{j,t+s}}{p_{t+s}} - \varepsilon_{p,t+s}mc_{t+s}y_{j,t+s} - \mathcal{C}^p_{j,t+s}\right)\right\}, \tag{13}$$

subject to the demand equation $y_{j,t} = l_t^{-1}\left(p_{j,t}/p_t\right)^{-\zeta}y_t$. $\Omega_{t,t+s} = (\beta(1-\vartheta))^s\frac{\lambda_{t+s}}{\lambda_t}$ is the stochastic discount factor that converts future payoffs into current values, and λ_t is the Lagrange

multiplier associated with the budget constraint of households. $\varepsilon_{p,t}$ is a cost-push shock that follows an AR(1) process: $\varepsilon_{p,t} = (1-\rho_p) + \rho_p \varepsilon_{p,t-1} + \eta_{p,t}$, where $\eta_{p,t} \sim \mathcal{N}(0, \sigma_p^2)$.

Since all intermediate goods firms face the same profit-maximizing problem, they set the same price $p_{j,t} = p_t$. In a symmetric equilibrium, where the expected survival rate from t to $t+s$ is given by $(1-\vartheta)^s$, the optimal pricing rule implies:

$$\kappa\left(\pi_t - \pi_t^\star\right)\pi_t = \kappa \mathbb{E}_t\left\{\Omega_{t,t+1}\left(\pi_{t+1} - \pi_{t+1}^\star\right)\pi_{t+1}\frac{y_{t+1}}{y_t}\frac{l_t}{l_{t+1}}\right\} + \zeta\varepsilon_{p,t}mc_t + (1-\zeta). \tag{14}$$

This equation represents the New Keynesian Phillips curve, which relates current inflation to the discounted sum of marginal costs.

2.3. **Public sector.** We apply both a unified fiscal rule and a unified monetary policy rule at the global level.[7] In particular, adopting a global monetary policy rule is a pragmatic modeling shortcut. While monetary frameworks differ across countries, most central banks today pursue inflation targeting regimes and operate in environments shaped by common global forces. Empirical evidence shows that real and financial cycles are increasingly synchronized across advanced economies (Rey, 2015), and global inflation dynamics are closely linked to oil, energy, and commodity prices, all inherently international in nature. The global dimension of supply chains and production networks further amplifies these linkages, with recent research documenting the emergence of a global Phillips curve driven by international input-output connections (Auer et al., 2017). As a result, policy rates across central banks exhibit substantial co-movement, and many economies face similar structural trends, such as declining natural interest rates and persistently low inflation. Given the global nature of climate change and its macroeconomic spillovers, using a unified monetary policy rule is a reasonable simplification. It enables us to capture key interactions between monetary policy and the green transition, while preserving the core insight that central banks' actions are shaped not just by domestic, but also by international developments. In this context, a unified rule structure enhances the tractability and transparency of the model without losing sight of the broader global dynamics at play.

Given these considerations, it is reasonable to assume a unified global monetary policy rule. Global forces increasingly shape the two core targets of central banks,inflation and output, leading to strong co-movements in policy rates across countries. In our model, monetary policy is represented accordingly by a Taylor-type rule, where the short-term nominal interest rate is gradually adjusted in response to deviations of inflation and output from their

[7] A multi-country coordination framework represents a natural extension of the model, enabling the analysis of additional effects arising from cross-country heterogeneity in economic structure, idiosyncratic business cycles, fiscal capacity, or exposure to climate risks. However, such an extension goes beyond the scope of our current analysis, which focuses on global aggregates to highlight the core macro-climate policy trade-offs.

respective targets:

$$\frac{r_t}{r} = \left(\frac{r_{t-1}}{r}\right)^{\phi_r} \left[\left(\frac{\pi_t^\star}{\pi}\right)\left(\frac{\pi_t}{\pi_t^\star}\right)^{\phi_\pi}\left(\frac{y_t}{y_t^\star}\right)^{\phi_y}\right]^{1-\phi_r} \varepsilon_{r,t}, \tag{15}$$

where r is the steady-state nominal interest rate, and $y_t^\star$ is the natural output, defined as the output that would prevail in imperfectly competitive markets but with flexible prices. The parameters ϕ_r, ϕ_π, ϕ_y capture the degree of interest-rate smoothing and the responsiveness of the policy rate to the inflation and output gaps, respectively. Finally, $\varepsilon_{r,t}$ is a monetary policy shock that follows the process: $\varepsilon_{r,t} = (1-\rho_r) + \rho_r \varepsilon_{r,t-1} + \eta_{r,t}$, with $\eta_{r,t} \sim N(0, \sigma_r^2)$.

Similarly, the fiscal rule captures a stylized representation of global fiscal coordination, wherein short-term bonds are issued at the global level, and all revenues from the carbon tax are redistributed to households on a lump-sum basis:

$$\int_0^{l_t} b_{i,t}\mathrm{d}i + \tau_{e,t}\int_0^{l_t} e_{j,t}\mathrm{d}j = \frac{r_{t-1}}{\pi_t}\int_0^{l_t} b_{i,t-1}\mathrm{d}i + \int_0^{l_t} \Pr\left(z_{i,t}=1\right) T_{i,t}^e \mathrm{d}i. \tag{16}$$

2.4. **Aggregation.** First, we aggregate consumption for the two types of households:

$$l_t c_t = \int_0^{l_t} \Pr\left(z_{i,t}=0\right) c_{L,t}\mathrm{d}i + \int_0^{l_t} \Pr\left(z_{i,t}=1\right) c_{H,t}\mathrm{d}i, \tag{17}$$

which leads to:

$$c_t = \omega c_{L,t} + (1-\omega)\, c_{H,t}. \tag{18}$$

It is assumed that bonds are in zero net supply:

$$\int_0^{l_t} b_{i,t}\mathrm{d}i = 0. \tag{19}$$

As discussed by McKay et al. (2017), as long as $c_{L,t} < c_{H,t}$, the Euler equation for the low-productivity worker does not bind with equality, since the right-hand side will always be less than the left-hand side. Therefore, let $\lambda_t = \varepsilon_{b,t} c_{H,t}^{-\sigma_c} = \varepsilon_{b,t}\left(\frac{c_t - \omega d_t}{1-\omega}\right)^{-\sigma_c}$ denote the marginal utility of consumption of high-productivity households. The *aggregate* Euler equation is then given by:

$$\lambda_t = \mathbb{E}_t\left\{\frac{\tilde{\beta}_{t,t+1} r_t}{\pi_{t+1}}\left((1-\omega)\lambda_{t+1} + \omega\varepsilon_{b,t+1} d_t^{-\sigma_c}\right)\right\}. \tag{20}$$

In contrast, the general equilibrium condition for hours worked is:

$$(1-\omega)\, n_t = n_t^d. \tag{21}$$

Finally, the resource constraint is given by:

$$y_t = l_t c_t + \frac{\kappa}{2}\left(\pi_t - \pi_t^\star\right)^2 y_t + \theta_{1,t}\mu_t^{\theta_2} y_t + \vartheta \Pi_t. \tag{22}$$

where Π_t represents the profits consumed by the fraction ϑ of firms exiting the market.

2.5. **Final system.** The final system can be summarized by the following set of four core equations, which determine: *(i)* detrended GDP ($\tilde{y}_t = y_t/(l_t z_t)$), *(ii)* the nominal interest rate (r_t), *(iii)* the inflation rate (π_t), and *(iv)* the cumulative stock of carbon emissions (m_t).

(1) *Investment-Saving (IS) curve:*

$$\left(\frac{x_t\tilde{y}_t - \omega\tilde{d}_t}{1-\omega}\right)^{-\sigma_c} = \beta\mathbb{E}_t\left\{\frac{\varepsilon_{b,t+1}}{\varepsilon_{b,t}}\frac{r_t}{\pi_{t+1}}\left((1-\omega)\left(\frac{x_{t+1}\tilde{y}_{t+1} - \omega\tilde{d}_t}{1-\omega}\right)^{-\sigma_c} + \omega\tilde{d}_t^{\,-\sigma_c}\right)\right\},$$

where $x_t = 1-(1-\vartheta)\frac{\kappa}{2}\left(\pi_t - \pi_t^\star\right)^2 - \theta_{1,t}\tilde{\tau}_{e,t}^{\theta_2/(\theta_2-1)} - \vartheta(1-\varepsilon_{p,t}mc_t)$ and $\tilde{d}_t = d\Phi\left(m_t\right)$;

(2) *Phillips Curve (PC):*

$$\left(\pi_t - \pi_t^\star\right)\pi_t = (1-\vartheta)\beta\mathbb{E}_t\left\{\left(1+g_{z,t+1}\right)\frac{\tilde{y}_{t+1}}{\tilde{y}_t}\left(\pi_{t+1} - \pi_{t+1}^\star\right)\pi_{t+1}\right\} + \frac{\zeta}{\kappa}\varepsilon_{p,t}mc_t + \frac{1-\zeta}{\kappa},$$

where $mc_t = \frac{\psi}{(1-\omega)^{\sigma_c+\sigma_n}}\frac{\left(x_t\tilde{y}_t - \omega\tilde{d}_t\right)^{\sigma_c}\tilde{y}_t^{(1+\sigma_n)/\alpha-1}}{\Phi(m_t)^{(1+\sigma_n)/\alpha}} + \theta_{1,t}\tilde{\tau}_{e,t}\left[\theta_2 + (1-\theta_2)\,\tilde{\tau}_{e,t}^{\frac{1}{\theta_2-1}}\right]$;

(3) *Monetary Policy (MP) rule:*

$$\frac{r_t}{r} = \left(\frac{r_{t-1}}{r}\right)^{\phi_r}\left[\left(\frac{\pi_t^\star}{\pi}\right)\left(\frac{\pi_t}{\pi_t^\star}\right)^{\phi_\pi}\left(\frac{\tilde{y}_t}{\tilde{y}_t^\star}\right)^{\phi_y}\right]^{1-\phi_r}\varepsilon_{r,t};$$

(4) *Climate Change (CC) curve:*

$$m_t - m_{t-1} = \xi_m\sigma_t\left(1-\tilde{\tau}_{e,t}^{\frac{1}{\theta_2-1}}\right)z_t l_t\tilde{y}_t\varepsilon_{e,t}.$$

In addition, the model includes five exogenous trends $\{z_t, \theta_{1,t}, l_t, \sigma_t, \pi_t^\star\}$ and four AR(1) shocks $\{\varepsilon_{b,t}, \varepsilon_{p,t}, \varepsilon_{r,t}, \varepsilon_{e,t}\}$.[8]

3. Bayesian inference

In this section, we estimate the model using Bayesian methods, using quarterly global data spanning from 1985Q1 to 2023Q2. The posterior distribution associated with the vector of observable variables is computed numerically using a Markov Chain Monte Carlo sampling approach.[9] Specifically, the Metropolis-Hastings algorithm enables efficient exploration of

[8] Appendix A in the Online Appendix provides the complete set of equations, including the shock processes and structural trends.

[9] We obtain a random draw of size 160,000 from the posterior distribution of the model parameters. This is achieved though eight parallel chains, each running 20,000 iterations, with a common jump scale parameter calibrated to obtain an acceptance rate of approximately 30%).

the high-dimensional parameter space efficiently, yielding a posterior distribution that explicitly accounts for parametric uncertainty, i.e., the uncertainty in parameter estimates arising from data limitations and model specification. Rather than relying on point estimates, this approach generates a distribution of potential parameter values, offering a more comprehensive view of the model's implications. By incorporating uncertainty into the parameter estimates, we capture a broader range of possible economic dynamics and assess the robustness of model-based predictions. We begin by describing how the nonlinear model with trends is solved, followed by a discussion of the selected data and our choice of priors, before commenting on the posterior distribution of the structural parameters.

3.1. **Numerical solution method with stochastic growth.** To solve the model, we address two key challenges: inherent nonlinearities in climate dynamics and unbalanced growth induced by five structural trends: rising population, output, and carbon emissions, alongside declining abatement efficiency and inflation targets.[10] We adapt the *extended path* solution method of Fair and Taylor (1983) and Adjemian and Juillard (2014) to account for the presence of growth in our model, avoiding the limitations of local solution techniques. The extended path method relies on a perfect foresight solver to compute paths for endogenous variables consistent with the model's equations, given a sequence of exogenous MIT shocks and the absence of aggregate uncertainty. While the classical extended path assumes convergence to a fixed steady state once shocks dissipate, our implementation instead allows convergence to a nonstationary deterministic transition path, reflecting the persistent structural trends embedded in the model. The advantage of this method is that it delivers an accurate and computationally efficient solution while accounting for all model nonlinearities.[11]

Taking nonlinear models to the data presents challenges, as nonlinear filters, necessary for forming the likelihood function, are computationally demanding. The inversion filter offers a computationally efficient alternative (see Guerrieri and Iacoviello, 2017). Originally introduced by Fair and Taylor (1983), the inversion filter recursively extracts the sequence of innovations by inverting the observation equation, given a set of initial conditions. Unlike the Kalman or particle filters, it relies on an analytical characterization of the likelihood function.[12] The inversion filter builds on the perfect foresight solution proposed by Juillard (1996), implemented in Dynare (Adjemian et al., 2024). The standard approach involves computing

[10] These trends are fundamental for accurately assessing climate change effects but render traditional perturbation methods unsuitable, as local approximations (e.g., around a deterministic steady state) break down.

[11] Appendix B in the Online Appendix provides additional details on the general representation of the perfect foresight algorithm in the presence of extended path, and the underlying statistical model used to estimate forward-looking models with structural changes.

[12] For a discussion of alternative filters for likelihood computation, see Fernández-Villaverde et al. (2016). See also Cuba-Borda et al. (2019) for detailed comparisons of inversion filter performance.

the dynamic path of variables given current and future shocks. Within the extended path framework, the inversion filter *(i)* substitutes current shocks and selected endogenous variables into the perfect foresight solution, and *(ii)* recovers current shocks and non-observable variable paths consistent with the observed data. Finally, we use the Metropolis-Hastings algorithm to sample from the posterior distribution and account parameter uncertainty.[13]

3.2. **Data description.** As some time series are not available on a quarterly basis, appropriate transformations are required. First, annual GDP in constant 2015 US$ is sourced from the *World Bank* (https://short-link.me/11hzB) and quarterly interpolated using the method of Chow and Lin (1971). This procedure relies on real quarterly GDP for total OECD countries from the *OECD Economic Outlook* database (https://short-link.me/15rfm) as the high-frequency indicator.[14] Quarterly headline inflation (https://short-link.me/15reP) and short-term nominal interest rates (https://short-link.me/11hyb) are also taken from the *OECD Economic Outlook* database. The aggregate interest rate is constructed by weighting national interest rates by their respective shares of OECD GDP. Annual CO_2 emissions, measuring emissions from fossil fuel combustion and cement production, are obtained from *Our World In Data* (https://short-link.me/11hzb). These data are also converted to quarterly frequency using the same Chow-Lin disaggregation approach applied to GDP. Our solution method explicitly accounts for the presence of trends in the data and therefore does not require variables to return to the steady state.[15] Consequently, we use the growth rate (i.e., the first difference of the logarithm) for GDP and CO_2 emissions, while maintaining the levels of inflation and nominal interest rates.[16] The measurement equations linking the model to the four macroeconomic and climate-related times series are given by:

$$\begin{bmatrix} \text{Real output growth rate} \\ \text{Inflation rate} \\ \text{Short-term interest rate} \\ \text{CO}_2 \text{ emissions growth rate} \end{bmatrix} = \begin{bmatrix} \Delta \log (y_t) \\ \pi_t - 1 \\ r_t - 1 \\ \Delta \log (e_t) \end{bmatrix}. \tag{23}$$

[13] The codes are part of a dedicated toolbox that builds on and extends the standard Dynare package (Adjemian et al., 2024), and are publicly available here: https://github.com/Vermandel/Climate-Economics-Dynare.

[14] This temporal disaggregation technique establishes a statistical relationship between low-frequency data and higher-frequency indicator variables. The method involves estimating regressions at the low-frequency level and applying the resulting coefficients to the indicator variables to construct a quarterly version of the target series.

[15] Linearization methods typically approximate a model's decision rules around a fixed point, effectively assuming stationarity in a neighborhood around the steady state. As a result, inference under such methods requires transforming the data to make it stationary (e.g., per capita scaling, detrending, or applying business cycle filters).

[16] Appendix C in the Online Appendix displays the times series of all observable variables used in the model.

3.3. **Calibrated parameters.** A first set of parameters is calibrated and can be grouped into two categories: structural parameters and initial conditions. We begin by discussing the calibration of the structural parameters, which are reported in Panels A and B of Table 1.

These parameters are categorized into three panels. Panel A pertains to the climate dynamics. The parameter ξ_m converts CO_2 to carbon units (GtC = ξ_m $GtCO_2$), ensuring consistency with climate damages measured in terms of cumulative carbon emissions. The parameter γ, which governs the impact of climate damages on total factor productivity (TFP), is set to 3.6×10^{-5}. This value implies a permanent 5% reduction in TFP under a business-as-usual scenario, in line with the recent calibration proposed by Barrage and Nordhaus (2024). This value is higher than that used in Golosov et al. (2014), reflecting the fact that damages in the DICE 2023 model are almost twice as large as those in its 2016R2 version. For the remaining parameters of the panel, we follow Barrage and Nordhaus (2024). The abatement cost function curvature, θ_2, is set to 2.6 to ensure strong convexity. Technological progress in the abatement sector, δ_{pb}, is calibrated to reduce abatement costs by 1.7% annually. In contrast, the decay rate of carbon decoupling δ_σ, is set to zero.

TABLE 1. Calibrated parameter values and initial conditions (quarterly basis)

NAME		VALUE	NAME		VALUE
Panel A: Climate parameters					
Atmospheric conversion factor	ξ_m	3/11	Long-term inflation target	$\pi^\star_\infty$	0.0025
Climate damage elasticity	γ	3.57e-05	Decay TFP (annualized)	δ_z	0.0018
Abatement cost curvature	θ_2	2.6			
Decay abatement cost	δ_{pb}	0.017/4			
Decay rate emission intensity	δ_σ	0	**Panel C: Initial conditions**		
			Initial GDP (trillion USD PPP)	y_{t_0}	7.5
Panel B: Economic parameters			Initial inflation trend (annualized)	$\pi^\star_{t_0}$	10/400
Firm exit probability	ϑ	0.05	Initial emissions ($GtCO_2$)	e_{t_0}	5.075
Unemployed payoff-to-consumption	d/c	0.97	Initial abatement cost-to-gdp	θ_{1,t_0}	0.3191
Share low productive workers	ω	0.02	Initial population (billion)	l_{t_0}	4.85
Terminal population (billion)	l_∞	10.48	Initial stock of carbon (GtC)	m_{t_0}	719.9
Population growth	l_g	0.025/4	Initial carbon price ($/ton)	τ_{e,t_0}	0
Goods substitution elasticity	ζ	4	Initial hours worked	h_{t_0}	1
Labor intensity	α	0.7	Initial interest rate	r_{t_0}	5/400

Note: $t_0 = 1984Q4$.

Panel B presents the calibration of the economic parameters. For discounting in the Euler and Phillips curves, the firm exit rate ϑ is set at 5%, consistent with the firm entry and exit literature and OECD data on firm death rates in the manufacturing and services sectors. In contrast, the Euler discount depends on the parameters ω and d. Following McKay et al. (2017), we calibrate the model to produce an effective discount rate of 3% by assuming

that 2% of workers experience an income shock, and that insurance covers 97% of their consumption. Regarding population dynamics, the initial population at the start of the sample (1984Q4) is set at 4.85 billion. It is assumed to converge toward a long-term population level of $l_\infty = 10.48$ billion at an annual rate of 2.5%, consistent with United Nations projections for the year 2100. The substitutability across intermediate goods implies a 33% markup, a standard value in macroeconomic models featuring imperfect competition. Finally, the growth decay parameter δ_z is taken from the DICE 2023 model.

Panel C reports the initial conditions required to pin down all state variables of the model prior to estimation at $t_0 = 1984Q4$. Labor supply is normalized to one, and labor intensity is set to 0.7, consistent with the DICE model. For the exogenous inflation target process, we minimize the difference between the model and observed inflation data. This yields an initial inflation target of 10% annually, which decays at a rate of 7.5% per year toward a long-run target of 1%. To ensure realistic levels for GDP and CO_2 emissions, we set initial GDP to 7.5 trillion USD and emissions to 5 $GtCO_2$, in line with 1984 data. The initial values of population, GDP, interest rate, and emissions are all set to their observed levels in 1984Q4. Based on atmospheric carbon concentration data, we set the initial carbon stock m_{t_0} to 719 GtC. From these values, we compute the implied damages and calibrate the initial level of hours worked to determine the disutility of labor parameter ψ. Given the initial GDP y_{t_0}, we use the production function to derive the initial level of total factor productivity, z_{t_0}. The level of the abatement cost function θ_{1,t_0} is calibrated following Barrage and Nordhaus (2024), who set abatement costs to reach 10.9% of GDP in 2020 under full abatement ($\mu = 1$). Since our simulation begins in 1984, we extrapolate this value backward, resulting in an estimated cost share of approximately 31.9% of GDP at t_0. For the initial carbon stock in our simulation, we again use the 1984 value of 719 GtC, based on historical concentration data.

The final variable requiring discussion is the expected path of the carbon tax $\tilde{\tau}_{e,t}$. The out-of-sample transition scenario influences agents' expectations, which in turn affects the data representation captured by the estimated model. Rather than imposing an arbitrary mitigation path (such as strict adherence to the Paris Agreement), we allow the data to inform the expected carbon tax trajectory. Let $\{\tilde{\tau}^\star_{e,t}\}^T_{1984Q4}$ denote the benchmark carbon tax path consistent with temperature stabilization by 2050, as targeted in the Paris Agreement.[17] Recognizing that agents may not fully believe in the realization of this mitigation path, we introduce an expectation formation mechanism: $\mathbb{E}_{t,t+S}\{\tilde{\tau}_{e,t}\} = \varphi\tilde{\tau}^\star_{e,t}$, where $\varphi \in [0,1]$ captures the degree

[17] Formally, the Paris Agreement-consistent tax path is assumed to increase linearly from 2023Q3 to 2050Q1, starting at 0$ per ton of carbon and reaching 152$ per ton, consistent with the backstop price under a full mitigation policy. After 2050, the carbon price declines endogenously due to decreasing cost of abatement $\theta_{1,t}$ and carbon intensity σ_t, consistent with the DICE framework.

of belief in the policy scenario. The parameter φ can be interpreted as *(i)* the prior probability that the mitigation policy will be fully implemented, *(ii)* the fraction of agents who believe in the policy's realization, or *(iii)* the perceived stringency of the policy path.

TABLE 2. Prior and posterior distributions of structural parameters

		Prior Distribution			Posterior Distribution		
		Shape	Mean	Std	Mode	Mean	[5%:95%]
Panel A: Shock processes							
Standard deviation: preference shock	σ_b	$\mathcal{IG}_2$	0.002	0.0033	0.0276	0.0276	*[0.0233:0.0321]*
Standard deviation: price markup shock	σ_p	$\mathcal{IG}_2$	0.002	0.0033	0.0223	0.0221	*[0.0189:0.0256]*
Standard deviation: monetary policy shock	σ_r	$\mathcal{IG}_2$	0.002	0.0033	0.0008	0.0008	*[0.0007:0.0009]*
Standard deviation: carbon emission shock	σ_e	$\mathcal{IG}_2$	0.002	0.0033	0.005	0.005	*[0.0045:0.0055]*
Autocorrelation: preference shock	ρ_b	$\mathcal{B}$	0.5	0.1	0.6828	0.6862	*[0.6358:0.7304]*
Autocorrelation: price markup shock	ρ_b	$\mathcal{B}$	0.5	0.1	0.9816	0.9786	*[0.9666:0.9883]*
Autocorrelation: monetary policy shock	ρ_r	$\mathcal{B}$	0.5	0.1	0.478	0.5214	*[0.4714:0.5893]*
Autocorrelation: carbon emission shock	ρ_e	$\mathcal{B}$	0.5	0.1	0.961	0.9601	*[0.9451:0.9739]*
Panel B: Structural parameters							
Initial TFP growth	$g_{z,t_0} \times 400$	$\mathcal{G}$	1.5	0.5	1.9125	1.8991	*[1.8623:1.9376]*
Decay rate decoupling	$g_{\sigma,t_0} \times 400$	$\mathcal{G}$	1.5	0.5	1.2994	1.3131	*[1.2565:1.3757]*
Risk aversion	σ_c	$\mathcal{G}$	1.25	0.25	1.589	1.5692	*[1.3798:1.7665]*
Labor disutility	σ_h	$\mathcal{G}$	2	0.25	0.8422	0.7938	*[0.6256:0.9625]*
Rotemberg Cost	κ	$\mathcal{G}$	30	6	170.3791	166.229	*[149.8725:183.1776]*
Convergence rate of inflation target	$\rho_{\pi^\star}$	$\mathcal{B}$	0.02	0.01	0.0258	0.0256	*[0.0189:0.0331]*
Initial interest rate	$r_{t_0} \times 400$	$\mathcal{N}$	12	2	8.7468	8.6852	*[8.1798:9.2709]*
Monetary policy: smoothing	ρ	$\mathcal{B}$	0.85	0.08	0.8857	0.8762	*[0.8459:0.8999]*
Monetary policy: inflation	$(\phi_\pi - 1)$	$\mathcal{G}$	0.8	0.07	0.5042	0.5176	*[0.4514:0.6009]*
Monetary policy: output gap	ϕ_y	$\mathcal{G}$	0.04	0.005	0.0559	0.0565	*[0.0429:0.0713]*
Discount rate	$(\beta^{-1} - 1) \times 100$	$\mathcal{G}$	0.8	0.2	0.2238	0.2265	*[0.156:0.2846]*
Mitigation policy belief	φ	$\mathcal{B}$	0.5	0.2	0.4831	0.4744	*[0.2974:0.583]*
Log marginal data density							-2862.47

Note: $\mathcal{B}$ denotes the Beta, $\mathcal{G}$ the Gamma, $\mathcal{N}$ the Gaussian, and $\mathcal{IG}_2$ the Inverse Gamma (type 2) distributions. A total of 120,000 draws were used to compute the posterior mean and 90% confidence interval. $t_0 = 1985Q4$.

3.4. **Prior and posterior distributions.** The remaining parameters are estimated using priors reported in Table 2. For most structural and policy parameters, we follow the specification in Smets and Wouters (2007). The autoregressive coefficients of the shock processes are assigned Beta priors with a mean of 0.5 and a standard deviation of 0.1, providing a relatively informative prior. The prior for the labor supply elasticity parameter, σ_h, is taken directly from Smets and Wouters (2007) and specified as a Gamma distribution to ensure positivity. Similarly, the risk aversion parameter σ_c is given a Gamma prior with a mean of 1.25 and a standard deviation of 0.25. The Rotemberg price adjustment cost parameter κ uses a Gamma prior (mean 30, standard deviation 6), which is at the lower end of the range found in the literature. For the inflation reaction coefficient, a Gamma prior is imposed on $\phi_\pi - 1$ to satisfy the Taylor principle, and the output gap reaction coefficient ϕ_y is also assigned a relatively tight Gamma prior. The exogenous shocks are specified to follow an inverse gamma type 2 distribution, as in Christiano et al. (2014), with a prior mean of 0.002 and a standard deviation

of 0.0033. The annualized slopes of TFP growth and carbon decoupling are estimated using diffuse Gamma priors (mean 1.5, standard deviation 0.5), consistent with values typically found in DICE models. Finally, the mitigation belief probability φ is assigned a diffuse Beta prior with a mean of 0.5 and a standard deviation of 0.2, capturing a wide range of possible beliefs regarding policy credibility.

We next examine the posterior distributions generated by the Metropolis-Hasting sampler, reported as 90% confidence intervals in Table 2. The price mark-up shock exhibits the highest persistence, consistent with the findings of Smets and Wouters (2007). Notably, the pollution shock also shows substantial persistence, in line with the results of Jondeau et al. (2023). Initial productivity growth is estimated to be higher than typical values in DICE models. This is expected, given that our simulation begins in 1985, a period characterized by stronger TFP growth compared to the 2015-2020 window used in A similar pattern is observed for the carbon decoupling rate. Relative to Smets and Wouters (2007), our estimates imply a flatter labor supply curve, which in turn flattens the marginal cost schedule and dampens the sensitivity of inflation to fluctuations in hours worked. Additionally, the Rotemberg price adjustment cost parameter is estimated to be relatively high, indicating a relatively flat Phillips curve. This finding aligns with extensive evidence from the Great Moderation period. The estimated coefficients on Taylor rules are effectively in line Smets and Wouters (2007). Importantly, the model estimates that agents assigned a probability of approximately 48% to achieving the goals of the Paris Agreement.

An evaluation of the model's fit, including a comparison of empirical and model-implied moments, is provided in Appendix D in the Online Appendix. Generalized impulse response functions for the four shocks and a historical decomposition of detrended output, inflation, and the nominal interest rate are also included. Overall, the model captures the empirical dynamics of these key variables reasonably well.

4. The anatomy of greenflation and climateflation

In this section, we analyze how the phenomena of climateflation and greenflation may shape the global economy through 2100. Our analysis relies on long-term projections generated by the model under alternative climate policy scenarios. Rather than being purely illustrative, these simulations constitute genuine out-of-sample forecasts produced by a structurally estimated dynamic model. This approach ensures internal consistency by anchoring both the structural parameters and initial conditions in the data. We then decompose output and inflation into their macroeconomic and environmental components to isolate the key drivers of the transition.

4.1. **Long-term projections under CO2 emission scenarios.** We begin by presenting long-term projections from the model to illustrate potential trajectories for the global economy by 2100. To this end, we implement three alternative scenarios in Figure 1, which differ solely in the degree of effective policy implementation, captured by the parameter φ.[18] The first scenario (green) aligns with the SSP1-1.9 pathway from IPCC (2021), representing full implementation of the Paris Agreement ($\varphi = 1$). The second (red) follows the SSP3-7.0 pathway, where agents learn that no carbon tax will be enacted ($\varphi = 0$), resulting in continued emissions growth (*laissez-faire*). In both cases, agents revise their expectations following a policy surprise. The third scenario (blue) corresponds to the estimated tax path, in which agents experience no surprise; they act based on a previously anticipated carbon tax trajectory inferred from the data.[19] Importantly, this analysis focuses on the macroeconomic effects of climate change mitigation rather than the optimal design of carbon taxation, which is addressed in the robustness section.

In the absence of emission controls and with a zero carbon tax, the laissez-faire scenario leads to a continuous increase in climate damages, driven by the ongoing rise in cumulative emissions. This leads to a progressive decline in total factor productivity (TFP), natural output, and the natural real interest rate (Panels D and F). Although the economy begins recovering from the energy price shock recession in 2023, output soon falls below the technological neutral trend due to intensifying climate damages, causing GDP to decline by nearly 2% relative to trend. The anticipated weakening of demand (Panel A) further suppresses inflation (Panel B), pushing it below the baseline blue scenario.[20] In response, the central bank lowers the policy interest rate (Panel C). Recent empirical work further highlights the supply-side origins of climateflation. Baleyte et al. (2024) show, using long-run historical data, that climate-related shocks tend to raise inflation and dampen economic activity, much like classic supply shocks.

The economy evolves quite differently under the Paris Agreement scenario. Here, a gradually increasing carbon tax is implemented, reaching \$150 per ton of CO_2 emissions by 2050, sufficient to support the transition to a net-zero carbon economy (Panels G and H). Initially,

[18] In 2023Q3, agents receive information about the long-term carbon tax trajectory, which may take the form of a surprise shift in policy intensity—either toward the Paris Agreement with $\varphi = 1$, or toward laissez-faire with $\varphi = 0$.

[19] All forecasts are shaped by four main forces, which differ significantly from the typical shock analysis in New Keynesian models: (i) exogenous processes, based on their in-sample realizations; (ii) deterministic trends converging gradually to terminal states; (iii) the implemented carbon price policy; and (iv) the accumulation of atmospheric carbon, which causes permanent damage to the economy.

[20] Climate damages act as a persistent supply shock, an effect extensively studied in Nuño et al. (2024) with respect to monetary policy.

FIGURE 1. Model-implied projections based on alternative control rates of emissions

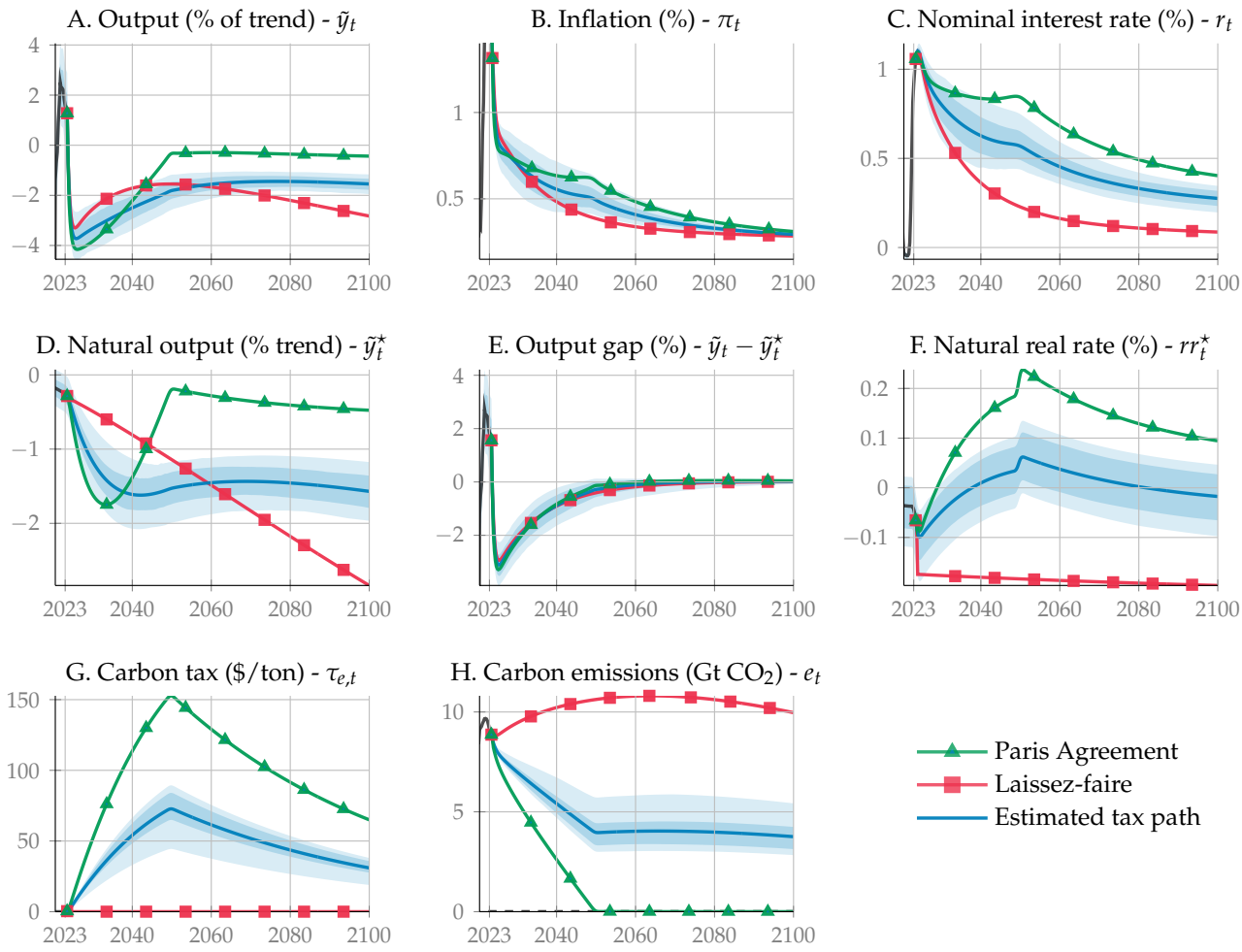

Note: This figure displays the projections of the main variables of the New-Keynesian climate model under three scenarios: *(i)* the Paris Agreement (carbon tax consistent with net zero in 2050), *(ii)* laissez faire (no carbon tax), and *(iii)* carbon tax consistent with the forecasts of the estimated model. The light blue area denotes the uncertainty band, derived from 500 random draws generated via the Metropolis-Hastings sampler.

natural output declines due to the rising tax burden and associated abatement costs. However, as abatement expenditures stimulate aggregate demand, output subsequently rises. The natural real interest rate follows a qualitatively similar pattern (Panel F). One notable consequence of this investment-led recovery is the emergence of more persistent inflationary pressures. While the output gap closes gradually under the laissez-faire scenario, it overshoots under the Paris Agreement path (Panel E).

Importantly, inflationary pressures persist even after net-zero is achieved in 2050. This reflects the continued economic costs associated with abatement investments, as captured in the DICE framework. These costs are modeled as flow expenditures, implicitly representing the amortized net present value of decarbonization efforts over the lifetime of the deployed capital or technology. The combined effects of rising carbon taxes and increased

abatement-driven demand generate a sustained inflationary impulse, a phenomenon we refer to as "greenflation". Consequently, monetary policy must tighten (Panel C) to manage these inflationary pressures. This result is supported by Fornaro et al. (2025), which show that accounting for endogenous technological change deepens the green dilemma for central banks: tolerating temporary inflation risks unanchoring expectations, while strict inflation targeting raises the economic cost of the transition by suppressing green investment and slowing progress toward sustainability. On empirical grounds, the inflationary effects of carbon taxation have been documented by Känzig and Konradt (2024) in the European context. The study finds that carbon taxes operate much like supply shocks, leading to higher inflation and a decline in real activity. This empirical evidence corroborates our findings regarding the emergence of greenflation in response to climate mitigation policies.

The deliberate simplicity of our model allows us to exploit its tractability to disentangle the most salient mechanisms that shape the transition. In particular, we perform a decomposition of aggregate demand and supply to identify the macroeconomic and environmental forces driving the dynamics of output and inflation, features common to a broad class of environmental macroeconomic models

4.2. **Decomposing output.** In this section we analyze the various forces that influence total output. From the resource constraint, the logarithm of detrended output, defined as $\hat{y}_t = \log(\tilde{y}_t/\tilde{y})$ can be approximated as follows:[21]

$$\hat{y}_t \simeq \underbrace{\widehat{IS}_t}_{\text{consumption}} + \underbrace{\theta_{1,t}\tilde{\tau}_{e,t}^{\theta_2/(\theta_2-1)}}_{\text{abatement expenditures}} + \underbrace{(1-\vartheta)\frac{\kappa}{2}(\pi_t-\pi_t^\star)^2+\vartheta(1-mc_t)}_{\text{nominal costs}}. \tag{24}$$

Three main forces can be identified in the decomposition of output. The first is $\widehat{IS}_t$, which captures the standard permanent income and intertemporal substitution effects on **consumption**.[22] This term also embodies the primary channel through which monetary policy operates. However, relative to the standard New Keynesian framework, its effect is attenuated due to the presence of discounting in the Euler equation. The second term represents **abatement expenditures**, autonomous abatement investment required to meet net-zero emission targets by 2050. These expenditures act as a source of aggregate demand, independent of

[21] Appendix E in the Online Appendix outlines the mathematical derivation of this approximation in detail.

[22] The attenuated IS has contribution $\widehat{IS}_t = \log(IS_t/IS)$ where attenuation coefficient $\omega \in [0,1]$ is given by $IS_t = \omega\tilde{d}_t + (1-\omega)\left[\omega\mathbb{E}_t\left\{\sum_{s=0}^{\infty}\beta(1-\omega)^s\varepsilon_{b,t+s}\tilde{d}_{t+s}^{-\sigma_c}\prod_{j=0}^{s}\frac{r_{t+j}}{\pi_{t+1+j}}\right\}\right]^{-1/\sigma_c}$.

monetary or fiscal stimulus. The third component, labeled **nominal costs**, reflects the resource costs associated with inflation, including menu costs and the consumption of dividends by firms exiting the market.

FIGURE 2. Decomposition of detrended output during the transition

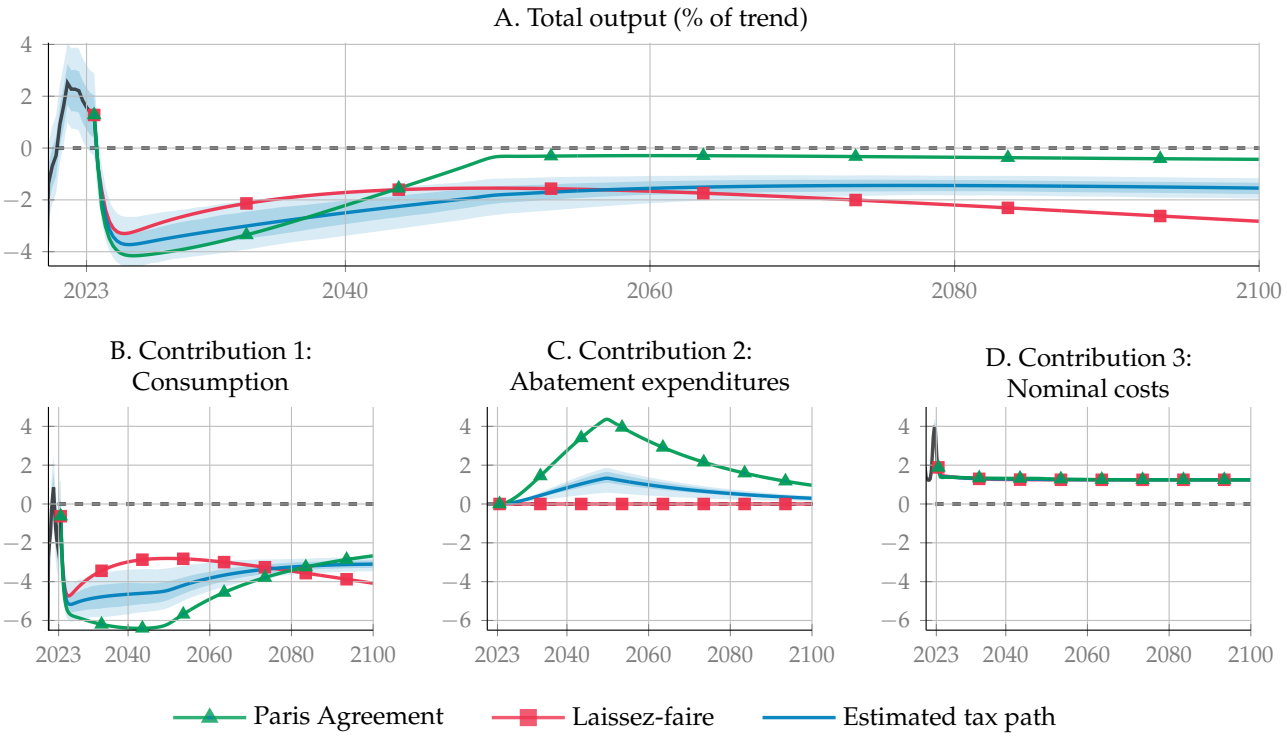

Note: This figure displays the projections of the detrended output under three scenarios: *(i)* the Paris Agreement (carbon tax consistent with net zero in 2050), *(ii)* laissez faire (no carbon tax), and *(iii)* carbon tax consistent with the forecasts of the estimated model. The light blue area denotes the uncertainty band, derived from 500 random draws generated via the Metropolis-Hastings sampler.

Figure 2 presents a decomposition of detrended output into three components across these scenarios. Note that Panel A shows total detrended output, which is the sum of the components shown in Panels B, C, and D. It is particularly insightful to compare the Paris Agreement scenario (green line) and the laissez-faire scenario (red line) with the baseline under the estimated carbon tax path (blue line). Under the Paris Agreement scenario, the rise in carbon taxes initially induces a deeper recession relative to the baseline, followed by a pronounced economic expansion as abatement spending intensifies, peaking at over 4% of output during the transition.[23] This initial downturn is primarily driven by negative supply-side effects, as

[23] Abatement costs in the model follow the structure of marginal abatement cost (MAC) curves, aligned with the DICE framework. These costs are modeled as the net present value of mitigation investments, implicitly distributed over time. Economically, this resembles a stream of coupon payments: while the initial investment reduces emissions, firms continue to incur annual costs over the lifetime of the deployed capital or technology. As a result, abatement spending persists beyond the point of achieving net-zero. Bilal and Känzig (2025)

higher taxes crowd out consumption (Panel B). In response to inflationary pressures arising from increased tax-induced production costs, monetary policy tightens. Notably, the inflationary burden (Panel D) remains relatively similar across all three scenarios, largely reflecting the persistent cost-push shock originating from the Ukraine war.

Conversely, the laissez-faire scenario yields a milder initial recession, as the absence of current and expected carbon taxes temporarily boosts output. Over time, however, rising climate damages reduce productivity, pushing output below baseline. Anticipating this deterioration in future economic conditions, forward-looking agents cut consumption in favor of precautionary savings, dampening inflation. Here, climate change transmits to output mainly through the intertemporal IS channel.

4.3. **Decomposing inflation.** We proceed in a similar manner to analyze the various forces that influence inflation. The Phillips curve in our framework exhibits strong nonlinearities. To preserve analytical tractability while capturing these essential features, we adopt a semi-linearization strategy.[24] This method enables a meaningful decomposition of the inflation gap, defined as $\hat{\pi}_t = \pi_t - \pi_t^\star$, into four main drivers:

$$\hat{\pi}_t \simeq \underbrace{\hat{\pi}_t^w}_{\text{real wage}} + \underbrace{\hat{\pi}_t^c}_{\text{climateflation}} + \underbrace{\hat{\pi}_t^g}_{\text{greenflation}} + \underbrace{\hat{\pi}_t^x}_{\text{cost-push shock}}, \tag{25}$$

with

$$\hat{\pi}_t^j = \frac{\xi - 1}{\kappa} \widehat{mc}_t^j + \mathbb{E}_t\{\beta_{t+1}^\pi \hat{\pi}_{t+1}^j\} \quad \text{for } j = \{w, c, g\},$$
$$\hat{\pi}_t^x = \frac{\xi - 1}{\kappa} \left(\varepsilon_{p,t} - 1\right) mc_t + \mathbb{E}_t\{\beta_{t+1}^\pi \hat{\pi}_{t+1}^x\},$$

where $\beta_{t+1}^\pi = (1 + g_{z,t+1})\, \tilde{y}_{t+1}/\tilde{y}_t$ is the discount factor adjusted by GDP growth, and $\widehat{mc}_t^j$ are the elements obtained from the linear approximation of the marginal cost expression:

$$mc_t = \underbrace{\frac{\psi \left(x_t \tilde{y}_t - \omega \tilde{d}_t\right)^{\sigma_c} \tilde{y}_t^{\frac{1+\sigma_n}{\alpha} - 1}}{(1-\omega)^{\sigma_c + \sigma_n}}}_{mc_t^w} \underbrace{\frac{1}{\Phi \left(m_t\right)^{\frac{1+\sigma_n}{\alpha}}}}_{mc_t^c} + \underbrace{\tilde{\tau}_{e,t} \theta_{1,t} \left(\theta_2 + \tilde{\tau}_{e,t}^{\frac{1}{\theta_2 - 1}} \left(1 - \theta_2\right)\right)}_{mc_t^g} \tag{26}$$

The term mc_t^w captures the standard component of marginal cost as in Galí (2008), driven by real wages through general equilibrium channels. The second term, mc_t^c, reflects the effects of

use MAC curves alongside regional carbon cost estimates to evaluate cost-effective unilateral decarbonization, finding that over 80% abatement is optimal for both the United States and European Union.

[24] We linearize only selected terms where necessary (e.g., components of marginal cost) while preserving key nonlinearities such as discount factors, the carbon tax channel, and climate damages. Each component's contribution to marginal cost is then translated into inflation dynamics through a nonlinear discounting mechanism. Appendix E in the Online Appendix outlines the mathematical derivation of this approximation in detail.

climate damages on production: as carbon emissions rise, total factor productivity declines, leading to higher marginal costs. This component is relatively exogenous, responding very moderately to endogenous variables such as output and inflation, and evolving largely in proportion to the carbon tax path. Finally, the term mc_t^g is linked to the implementation of the carbon tax and the associated abatement expenditures. It represents an additional source of cost pressure on firms and is entirely exogenous, determined solely by the degree to which the carbon tax is effectively realized.

Figure 3 illustrates the contribution of each component to the inflation gap under the three alternative scenarios. The overall dynamics of the inflation gap are broadly similar across scenarios, largely due to a disinflationary process driven by the dissipation of previously estimated positive cost-push shocks toward the end of the sample (Panel E). However, as discussed earlier, inflation is notably more persistent under the Paris Agreement scenario. By 2050, the inflation rate is approximately 0.3 percentage points higher (1.2 percentage points on an annualized basis) than under the laissez-faire scenario. This quantitative estimate of greenflation aligns closely with the findings of the large-scale model of Coenen et al. (2024), though it is significantly higher than the estimates reported in Olovsson and Vestin (2023). The decomposition shows that, under the Paris Agreement, the contribution of climateflation, that is, inflation stemming from the productivity-reducing effects of global warming, is lower than in the baseline scenario, stabilizing at around 0.6 percentage points toward the end of the century (Panel C). In contrast, the rise in carbon taxes and the associated abatement expenditures result in a substantially larger contribution from greenflation, which peaks at over 3 percentage points in 2030. A strong general equilibrium feedback from the wage-setting mechanism helps to partially offset these inflationary pressures. Specifically, the crowding-out of consumption due to increased abatement spending generates a wealth effect that increases labor supply, thereby inducing a significant decline in real wages. Nevertheless, this adjustment in real wages is insufficient to fully neutralize the inflationary pressures, ultimately resulting in a more inflationary environment under the Paris Agreement scenario.

In contrast, under the laissez-faire scenario, the contribution of climateflation ($\hat{\pi}_t^c$) steadily increases relative to the baseline, surpassing 5 percentage points by the end of the century as climate-induced productivity losses accumulate. However, this inflationary effect is more than offset by the negligible contribution of greenflation, which remains effectively zero throughout. While real wages initially decline less under laissez-faire, they become increasingly affected by persistent productivity deterioration stemming from unchecked global warming.[25] Importantly, we find that the general equilibrium feedback from wage dynamics

[25]Unlike standard decompositions in linearized models, typically based on orthogonal shocks, our nonlinear framework does not allow for a clean separation of inflation drivers. The contributions from greenflation and

FIGURE 3. Decomposition of inflation during the green transition

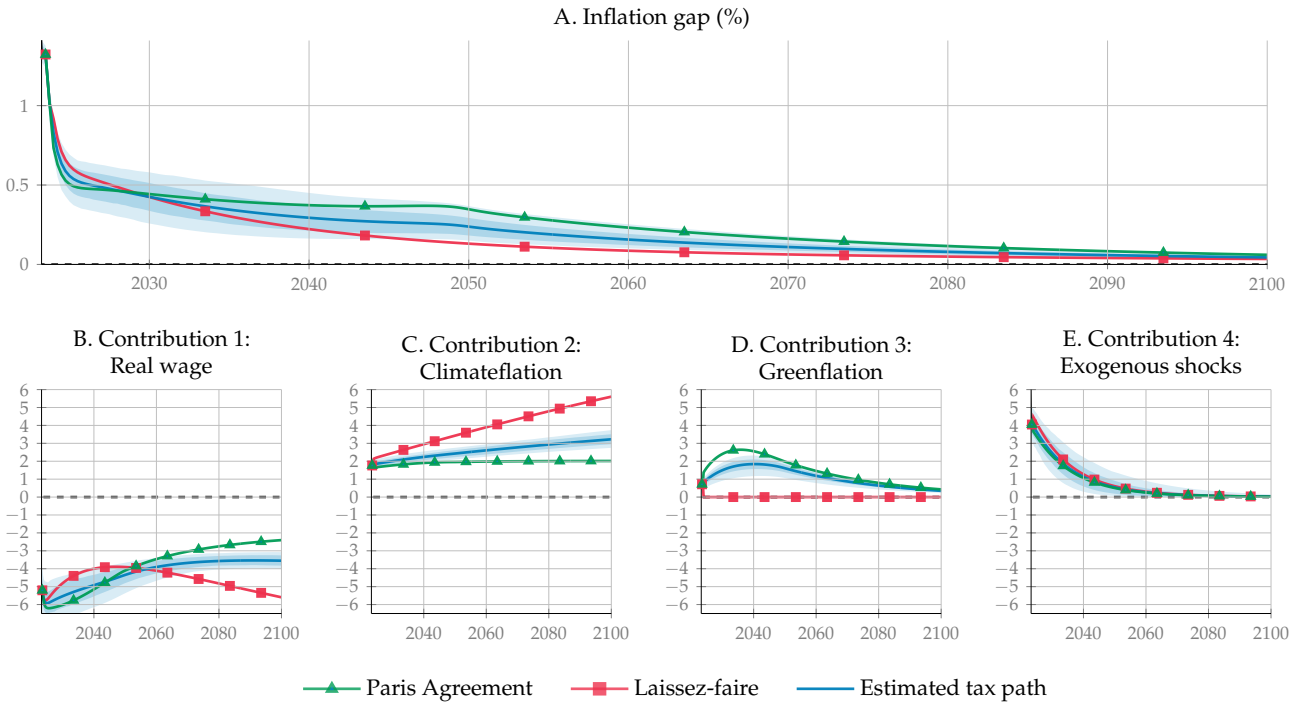

Note: This figure presents projections of the inflation gap, defined as inflation relative to its target, under three scenarios: *(i)* the Paris Agreement (carbon tax consistent with achieving net-zero emissions by 2050), *(ii)* laissez-faire (no carbon tax), and *(iii)* a carbon tax path consistent with the insample expectations derived from the estimated model. The light blue area denotes the uncertainty band, derived from 500 random draws generated via the Metropolis-Hastings sampler.

is sufficient to partially attenuate the effects of climateflation. In the robustness section of the paper, we explore how this wage adjustment mechanism is altered under varying degrees of wage stickiness.

In summary, our framework highlights a key result: stronger mitigation policies tend to be more inflationary, as the inflationary effects of greenflation outweigh the disinflationary effects from reduced climate damages (climateflation). The overall inflationary trajectory is therefore highly sensitive to how effectively real wages adjust, which determines the extent to which climate- and policy-induced cost pressures are absorbed. In the final section, we investigate how general equilibrium mechanisms (such as the role of capital in production, wage rigidity, and the redistribution of carbon tax revenues) shape this wage adjustment and, in turn, the inflationary response.

wage pressures are intertwined through general equilibrium interactions and cross-effects. As a result, they are not orthogonal: for example, $\text{cov}\left(\hat{\pi}t^{g}, \hat{\pi}t^{w}\right) \neq 0$. This implies that changes in one component, such as productivity losses from climate damages, can influence the relative weight of wage contributions to inflation.

4.4. **Parameter sensitivity analysis.** To assess how structural parameters shape inflation, output, and interest rates during the green transition, we perform a sensitivity analysis detailed in Appendix F in the Online Appendix. Specifically, we examine the effects of changes in the degree of discounting, the monetary policy reaction coefficients, the slopes of the aggregate demand and Phillips curves and key climate-related parameters. The results show that greenflation intensifies when: (i) households are less forward-looking; (ii) price setters are more forward-looking; (iii) the central bank responds weakly to inflation gap or strongly to output gap; (iv) the Phillips curve is steeper; and (v) the interest elasticity of consumption is lower. Higher abatement costs also raise inflationary pressures, while greater climate damages mainly affect long-run productivity with limited impact on transition-related inflation.

5. Climate change and monetary policy

This section explores the interaction between climate change and monetary policy, building on the extensive discussion in Schnabel (2022). In particular, it examines how the central bank's inflation–output trade-off is reshaped by the structural changes induced by climate change and associated mitigation policies. Additionally, it investigates how the design of the monetary policy rule modulates the broader macroeconomic impact of climate-related shocks and policy interventions.

5.1. **Managing the inflation/output tradeoffs in the presence of climate change.** Figure 4 illustrates how climate change and mitigation policies influence the central bank's trade-off between inflation and output stabilization. The figure plots the inflation-output variability frontier across two distinct time horizons and for two transition scenarios: (*Paris Agreement* and *laissez faire*). The first horizon corresponds to the medium run, defined as the transition period from 2024 to 2050, while the second captures the long run, covering the post-transition period from 2050 to 2100.

The figure illustrates how, during the transition period, the Paris Agreement scenario shifts the inflation/output variability frontier outward and to the right, relative to the laissez-faire scenario. This indicates a deterioration in the trade-off between inflation and output stabilization. Depending on its loss function, the central bank can opt to contain inflation volatility at the cost of greater output variability, or vice versa, but it cannot avoid the overall worsening of the trade-off during the transition. This finding is consistent with Del Negro et al. (2023), who identify similar dynamics in a multi-sector model, and resonates with the observations of Schnabel (2022), who emphasize the supply-driven nature of the greenflation shock.

FIGURE 4. Inflation-output variability frontier under alternative output gap weight in the Taylor rule

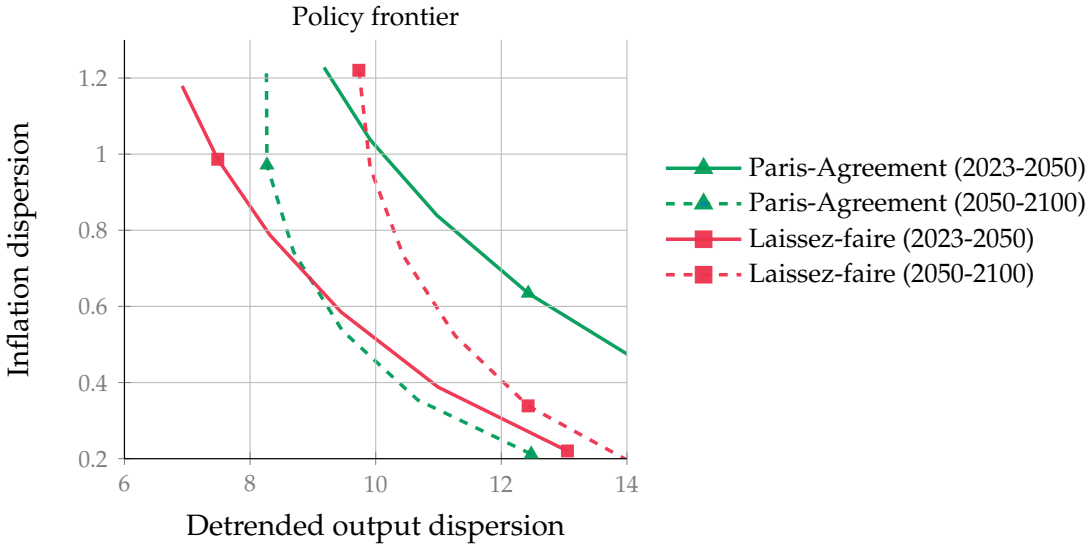

Note: This figure plots the dispersion of inflation (y-axis) against the dispersion of detrended output (x-axis) for varying values of the monetary policy response coefficient ϕ_y, under two scenarios: *(i)* the Paris Agreement (green) and *(ii)* laissez-faire (red). Inflation dispersion is measured as $\mathbb{E}\{(\pi_t - \pi_t^\star)^2\}$, while output dispersion is measured as $\mathbb{E}\{(\tilde{y}_t - \tilde{y})^2\}$. These dispersion metrics are computed by sampling shocks over 50 independent Monte Carlo chains. For each chain, the average squared deviation is calculated over a specified period (e.g., 2023Q1–2050Q2) and all 50 draws.

Importantly, the medium-term stabilization costs of climate mitigation are offset by a significantly improved trade-off in the long run. Post-transition, the inflation-output variability frontier under the Paris Agreement shifts inward, suggesting enhanced macroeconomic stability. While mitigation efforts impose short-term economic costs, particularly in the form of elevated inflation volatility, they also establish the foundation for a more stable environment in the second half of the century. In contrast, the laissez-faire path appears more favorable in the medium term, with lower volatility levels. However, the absence of climate policy ultimately results in significantly higher inflation and output dispersion in the long run, due to the compounding effects of climate damages.

In summary, this analysis underscores the trade-off between short-term costs and long-term benefits of climate mitigation. While the green transition may lead to higher inflation in the medium term, it significantly reduces GDP volatility over time, illustrating the dynamic intertemporal nature of climate-related monetary policy challenges.

5.2. **Natural rates and the design of the monetary policy rule.** As discussed in subsection 4.1, climate change and associated mitigation policies can significantly influence both the level and growth rate of natural output, as well as the natural short-term real interest rate $r^\star$, that is, the equilibrium real interest rate in an economy without nominal frictions.

Monetary policy rules typically rely on constant benchmarks, such as steady-state policy rate (or inflation target), as in standard DSGE models like Smets and Wouters (2007). However, when structural forces like climate change or transition policies induce persistent shifts in the natural rate of interest, relying on this assumption can lead to systematic policy errors. As emphasized by Orphanides (2002), misperceiving the natural rate can severely impair a central bank's ability to stabilize inflation and output. In what follows, we examine how this misjudgment may undermine monetary policy effectiveness, particularly during the transition to a low-carbon economy.

To this end, we specify the monetary policy rule as a general function of the pair $(\varsigma_{r,t}, \varsigma_{y,t})$, defined as:

$$\varsigma_{r,t} = \varsigma_{r,t-1}^{\phi_r} \left[\left(\frac{\pi_t^\star}{\pi} \right) \left(\frac{\pi_t}{\pi_t^\star} \right)^{\phi_\pi} \varsigma_{y,t}^{\phi_y} \right]^{1-\phi_r} \varepsilon_{r,t}. \tag{27}$$

We consider two alternative specifications of this rule. The first, denoted R_b, represents the estimated baseline rule and aligns with standard formulations in macroeconomic models. It is defined as follows:

$$(\varsigma_{r,t}, \varsigma_{y,t}) = \left(\frac{r_t}{r}, \frac{\tilde{y}_t}{\tilde{y}_t^\star} \right). \tag{28}$$

Here, the nominal interest rate is expressed relative to a constant long-run level, while output is measured against its time-varying natural counterpart, which accounts for climate-related effects. However, as explained above, this approach may inadvertently imply a return to a steady-state interest rate, even in the presence of structural changes driven by climate impacts of policy interventions.

Given that the same structural forces driving natural output also influence the natural interest rate (Laubach and Williams, 2003, Holston et al., 2017), anchoring monetary policy to a fixed long-run interest rate becomes problematic amid evolving conditions. As an alternative, we define the policy rule in terms of deviations from the time-varying natural interest rate. This specification, denoted $R_\star$, is given by:

$$(\varsigma_{r,t}, \varsigma_{y,t}) = \left(\frac{r_t}{r_t^\star \pi_t^\star}, \frac{\tilde{y}_t}{\tilde{y}_t^\star} \right). \tag{29}$$

Figure 5 illustrates the macroeconomic outcomes under both monetary policy rules. The rule that responds to both the natural output level and the natural real interest rate proves most effective in stabilizing inflation. Under both climate scenarios, it promotes a quicker convergence of inflation toward the 1% target, with only a modest increase in output volatility. By aligning policy with evolving natural rates, the central bank strengthens its capacity to stabilize the economy in the face of structural transformations induced by climate dynamics and mitigation measures.

FIGURE 5. The impact of climate transition under alternative monetary policy rules

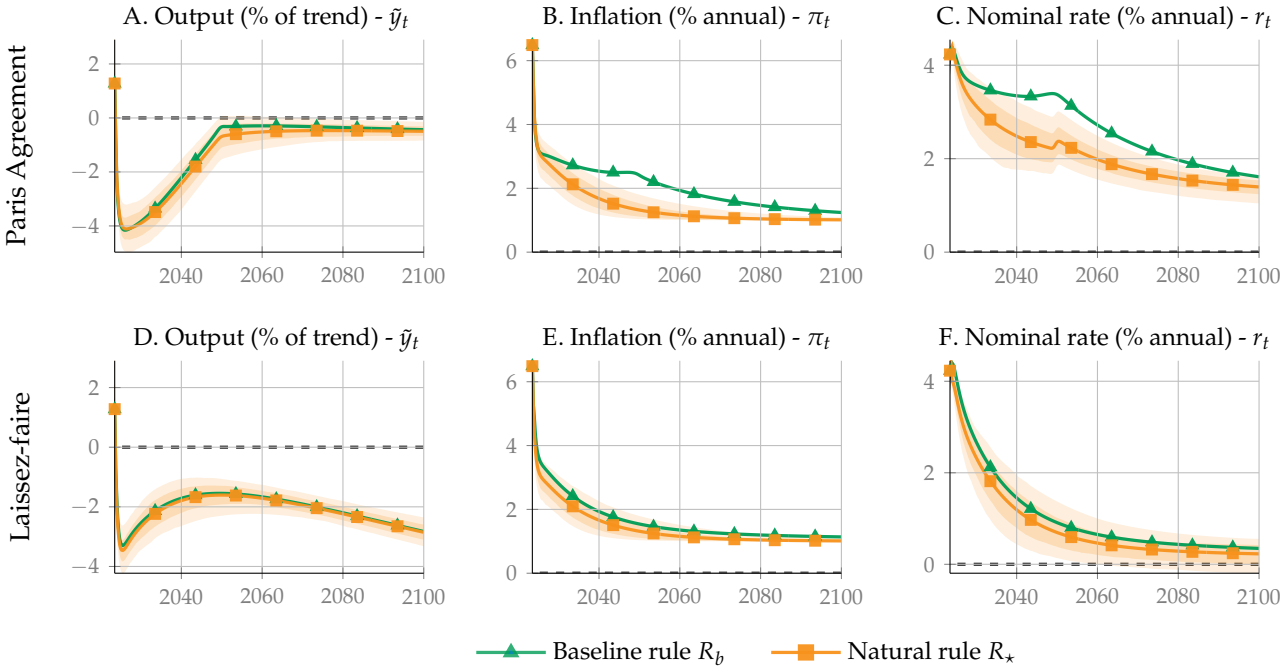

Note: This figure presents the trajectories of key variables under the Paris Agreement scenario for three different monetary policy rules: *(i)* the estimated policy rule (green line), where $(\varsigma_{r,t}, \varsigma_{y,t}) = (r_t/r, \tilde{y}_t/\tilde{y}_t^\star)$, and *(ii)* a natural-rate-adjusted rule (orange line), where $(\varsigma_{r,t}, \varsigma_{y,t}) = (r_t/(r_t^\star \pi_t^\star), \tilde{y}_t/\tilde{y}_t^\star)$. The light orange area denotes the uncertainty band associated with the natural-rate-adjusted rule, derived from 500 random draws generated via the Metropolis-Hastings sampler.

Conversely, when the policy framework disregards the effects of climate change and mitigation policies on natural output and interest rates, inflation remains persistently above target across the projection horizon. This issue is particularly acute under the Paris Agreement scenario, where structural shifts are more pronounced. However, even in the laissez-faire scenario, failing to account for the gradual decline in productivity due to climate damages results in higher inflation. These findings underscore the imperative of adapting monetary policy frameworks to the evolving macroeconomic environment shaped by climate change.

6. THE SOCIAL COST OF CARBON

This section analyzes the concept of the social cost of carbon (SCC) within the context of our New Keynesian framework. The SCC represents the monetary value of the economic damage caused by emitting one additional ton of carbon dioxide into the atmosphere. As such, it provides an optimal price for carbon emissions and serves as a key benchmark for policy evaluation and model comparison. We begin by calculating the SCC in the presence of nominal rigidities, and then examine the macroeconomic implications of aligning carbon pricing with this optimal trajectory.

6.1. **Pricing carbon in the presence of sticky prices.** This section assesses whether nominal price rigidities significantly affect the determination of the socially optimal carbon price. An approximation of the SCC can be formally expressed as:

$$SCC_t \approx \frac{\beta}{\lambda_t^c}\mathbb{E}_t\left\{\lambda_{t+1}^c SCC_{t+1} + 1000\xi_m l_{t+1} z_{t+1}^{1-\sigma_c}\gamma\frac{\psi}{\alpha}\left(\frac{n_{t+1}}{1-\omega}\right)^{1+\sigma_n}\right\}, \tag{30}$$

where $\gamma\frac{\psi}{\alpha}\left(n_{t+1}/\left(1-\omega\right)\right)^{1+\sigma_n}$ captures the marginal damage and λ_t^c is the marginal utility of consumption to express the SCC into consumption equivalents. This formulation is closely related to Golosov et al. (2014), with the key difference that nominal rigidities are embedded into the pricing kernel.

In our framework, the welfare cost of inflation appears directly through its impact on the marginal utility of consumption, which serves as the intertemporal pricing kernel. The marginal utility of consumption is defined as:

$$\lambda_t^c = \varepsilon_t^b\left(\frac{x_t y_t}{1-\omega} - \omega d_t\right)^{-\sigma_c},$$

where x_t, as a reminder, denotes the resources available for consumption after accounting for costs induced by both inflation and abatement efforts. When realized inflation persistently exceeds the central bank's target, particularly as a result of carbon taxes generating additional inflationary pressure, this amplifies the welfare cost of inflation by reducing x_t and, consequently, lowers agents' perceived wealth. In economic terms, the welfare cost of inflation manifests not only as a direct resource cost in the resource constraint, but also through its effect on the marginal utility channel: as agents feel poorer, their valuation of future welfare gains from abatement diminishes. Our analysis connects to Bailey (1956) and Lucas (2000), but it also resonates with insights from the fiscal theory of the price level (Leeper, 1991; Woodford, 1995; Cochrane, 2001). In contrast to standard monetary models where inflation is driven by monetary expansions, here inflation is primarily fiscal in origin, arising from persistent tax-induced shifts in the intertemporal government budget constraint. Accordingly, the welfare cost of "greenflation" has direct implications not only for monetary policy credibility, but also for the optimal path and timing of carbon pricing.

In Figure 6, we report the optimal carbon price in both the sticky price (nominal rigidity) and natural price (flexible price) economies, as well as uncertainty bands from 500 Metropolis-Hastings draws.[26] Once the transitory effect of shocks has dissipated, one observes that the

[26]Benchmarking our results against Barrage and Nordhaus (2024), we find that the level of the optimal carbon price in our model is broadly consistent with their main findings. However, direct comparison is complicated by important differences in model structure: our framework features behavioral discounting and nominal rigidities but omits both physical capital. As a result, the main source of persistence in our model is interest rate smoothing, which allows the optimal carbon tax to converge more rapidly to the SCC. In contrast, Barrage and

optimal carbon tax is, on average, higher in the natural economy: in the absence of nominal rigidities, the transition is not accompanied by persistent inflation, and the welfare cost of inflation remains lower. By contrast, under nominal rigidities, the social cost of carbon reflects a trade-off between nominal stability and climate objectives. If inflation is not stabilized during the green transition, the increased welfare cost of inflation diminishes the incentive for strong carbon pricing and thus lowers the optimal SCC. In other words, optimal climate policy becomes less ambitious whenever the transition generates sustained inflation above target, because agents discount future climate damages more heavily when their perceived wealth is eroded by inflationary distortions.

FIGURE 6. Pricing carbon at its social cost

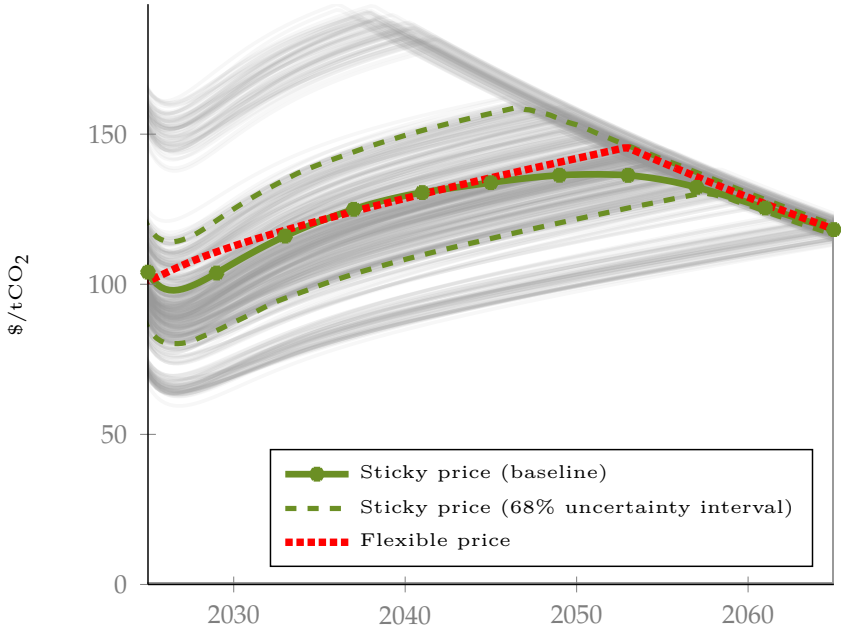

Note: This figure depicts carbon tax set to the social cost of carbon as derived from the estimated New Keynesian Climate model (green line) alongside its flexible-price (natural) counterpart (red dotted line). Uncertainty bands for the baseline, based on 250 simulations with alternative parameter draws from the Metropolis-Hastings algorithm, are shown as solid gray lines.

Nordhaus (2024) show that additional frictions result in a more gradual adjustment of the optimal carbon price toward the SCC. In our simulations, the optimal carbon price rises steadily and typically reaches the backstop price by 2060 in most Metropolis-Hastings draws. Our estimated carbon price also tends to be higher on average, reflecting our lower discount rate of 0.88%, which is estimated from global data and is lower than typical values used in DICE. This lower discount rate induces the planner to adopt a more aggressive carbon tax policy, accelerating the response to the climate externality. It is also worth noting that, across simulation draws, the optimal carbon price spans a wide range, from $50 to $160, encompassing the values reported in DICE and reflecting uncertainty associated with the estimated discount rate.

6.2. **The aggregate implications of carbon mispricing.** Standard IAMs, including those used by the IPCC, are typically constructed in a real framework that abstracts from nominal frictions such as sticky prices and monetary policy dynamics. As a result, the optimal SCC recommended by these models does not account for inflation or the welfare cost of inflation induced by carbon pricing.[27] In real-world policy settings, the SCC is thus computed from models that do not incorporate nominal rigidities. This raises an important question: what are the quantitative implications of applying such a mis-specified SCC in economies where nominal rigidities matter? To address this, we compute the SCC under both flexible-price and sticky-price environments. We then assess the macroeconomic implications of implementing a mis-specified SCC: specifically, applying an SCC derived under flexible-price assumptions (red dotted line in Figure 6) in an economy where nominal rigidities distort the transmission of climate policy.

We quantify the costs of such miscalibration along two key dimensions. First, we compare aggregate consumption paths under two regimes: one based on the flexible-price SCC and the other on the SCC optimized for the sticky-price environment (green line in Figure 6). The resulting difference, expressed in monetary terms (billions of dollars), reflects the real economic cost borne by households due to mispriced carbon tax. Second, we assess the inflation outcomes under both regimes to evaluate how a misaligned SCC impacts price stability. This comparison reveals the extent to which nominal rigidities amplify the inflationary effects of an ill-suited climate policy.

As shown in Figure 7, there are two main losses from applying an SCC derived from a flexible-price framework. It results in an average consumption loss of approximately $95 billion per quarter through 2050, with losses peaking at nearly $350 billion just before 2035. These figures are economically significant. On the inflation side, the average deviation is 0.04 percentage points, with short-term differences reaching up to 0.2 percentage points in annual terms. These results illustrate how the welfare cost of inflation materializes in this context. Because nominal rigidities slow the adjustment of prices, the economy is forced to absorb shocks primarily through quantities such as consumption and output, rather than through prices. This effect is especially pronounced when the SCC is calibrated from a natural (flexible-price) economy, as it does not account for the nominal distortions present in the real world. As a result, ignoring these nominal effects can lead to substantial welfare losses during the low-carbon transition.

[27] For example, the Biden administration in the United States set its central SCC at $52 per ton, based on a multi-model average derived from five leading IAMs. All of these models neglect inflationary effects and the welfare cost of inflation.

FIGURE 7. Macroeconomic costs of mispricing the social cost of carbon

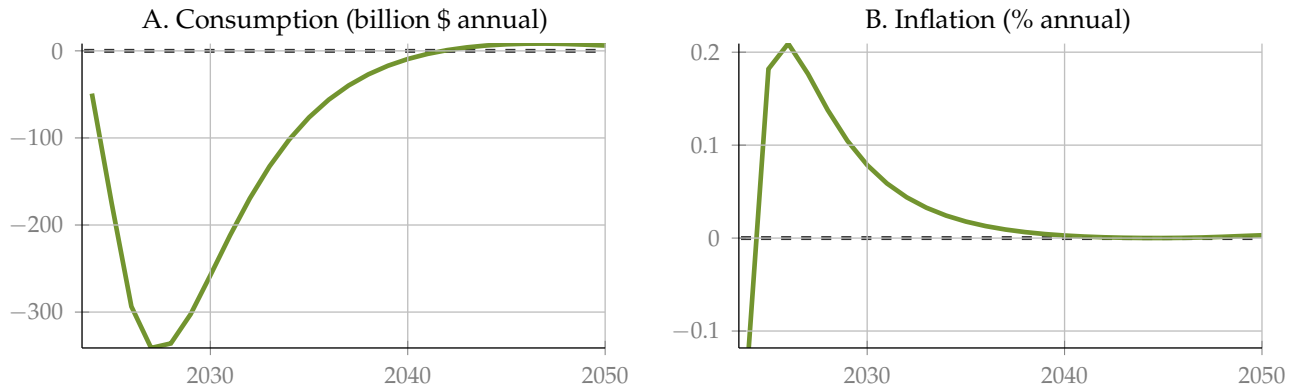

These findings have important policy implications. Nominal rigidities play a central role in shaping the macroeconomic consequences of carbon pricing. Yet current policy recommendations often rely on social cost of carbon estimates derived from models that abstract from these frictions. This oversight can weaken the effectiveness and public acceptance of climate policies. Recent episodes, such as the "yellow vest" protests in France, illustrate how public support for higher carbon prices can erode when such measures are perceived as fueling inflation and worsening cost-of-living conditions. Survey evidence confirms that individuals have a strong aversion to inflation and view its distributional effects as particularly unfair (Shiller, 1997; Di Tella et al., 2001), which can intensify opposition to climate interventions (Dechezleprêtre et al., 2025).

6.3. **The macroeconomic implications of adhering to optimal transition pathways.** In the baseline Paris Agreement scenario, the carbon tax is imposed exogenously and does not adjust optimally to maximize social welfare. Consequently, this approach is not directly comparable to integrated assessment models such as DICE, where the carbon price is determined endogenously to balance economic and environmental tradeoffs. To establish a more meaningful benchmark, we therefore compare the Paris Agreement carbon trajectory with two alternative optimal pathways: one based on the social cost of carbon, and another based on the optimal exhaustion of a fixed carbon budget. Under the Paris Agreement scenario, the atmospheric carbon stock is projected to increase by 100 GtC by 2050. For comparability with the scenario in Barrage and Nordhaus (2024), which targets limiting global warming to below 2°C, we also examine an alternative pathway in which a 100 GtC carbon budget is exhausted optimally over time.[28]

[28]The extraction rate for this scenario follows the optimal path defined by:

$$\max_{\{s_t\}} \mathbb{E}_t \left\{ \sum_{s=0}^{\infty} \tilde{\beta}_{t,t+s} \left(\frac{c_{t+s}^{1-\sigma_c} - 1}{1-\sigma_c} - \psi_{t+s} \frac{n_{t+s}^{1+\sigma_n}}{1+\sigma_n} \right) \right\} \quad \text{s.t.} \quad \Delta s_t = -\xi_m e_t.$$

Figure 8 compares the evolution of key macroeconomic and environmental variables under three distinct policy scenarios: *(i)* the Paris Agreement (green line), *(ii)* a carbon tax path aligned with the SCC (yellow line), and *(iii)* a carbon tax path consistent with the carbon-budget rule (purple line).

FIGURE 8. Alternative carbon tax trajectories

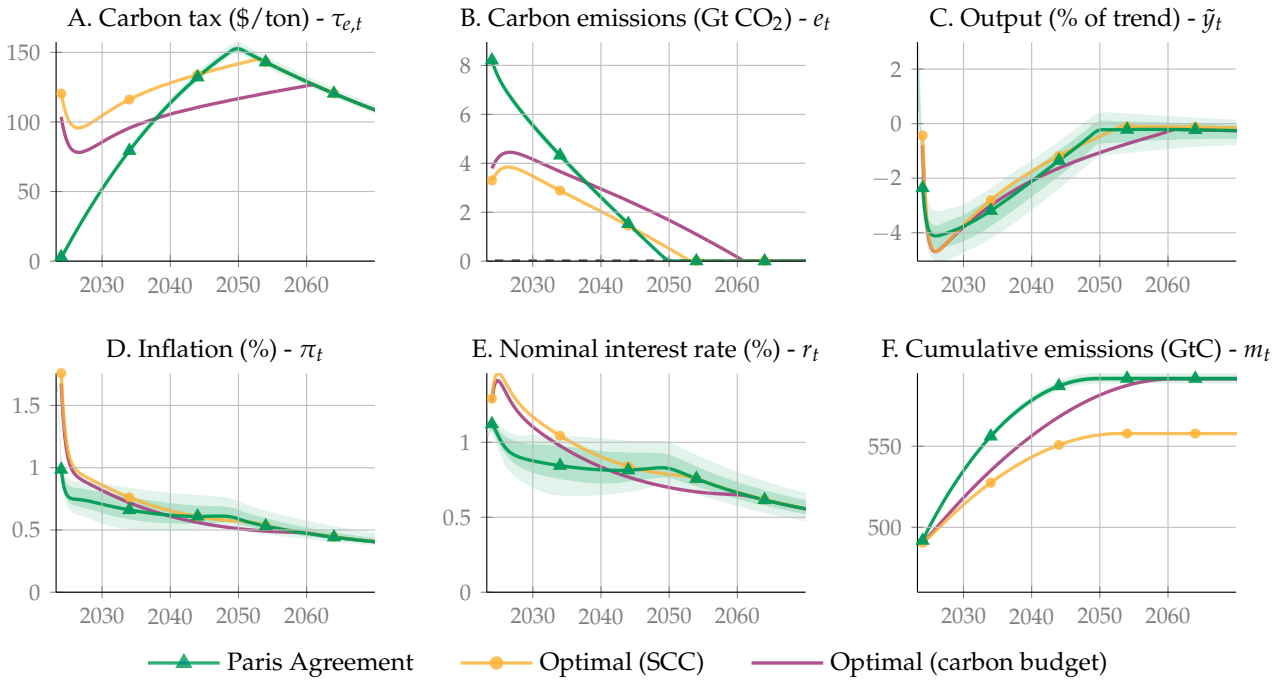

Note: This figure presents the projected paths of key macroeconomic and environmental variables under two scenarios within the New Keynesian climate model: *(i)* the Paris Agreement scenario, which assumes a carbon tax consistent with achieving net-zero emissions by 2050, and *(ii)* the optimal tax trajectory scenario, which reflects the optimal exhaustion of a fixed carbon budget. The green area denotes the uncertainty band associated with the Paris Agreement scenario, derived from 500 random draws generated via the Metropolis-Hastings sampler.

Under the SCC-based policy, it is optimal to emit approximately 50 GtC more than under the Paris Agreement. Although the carbon tax starts at a higher level in 2023, its growth rate is slower compared to the trajectories implied by the Paris Agreement or the carbon-budget rule. This leads to an initial spike in inflation, driven by the sudden increase in the carbon tax, but the resulting contraction in output is relatively modest. In this scenario, net-zero emissions are achieved by 2055. In contrast, the carbon-budget rule implies a more aggressive reduction in carbon emissions early in the transition. To meet the fixed carbon constraint, the carbon tax increases more rapidly, leading to stronger inflationary pressures, higher nominal interest rates, and a deeper short-term economic contraction. As a result, the atmospheric carbon stock rises more slowly over time.

This defines the optimal depletion path of the carbon stock s_t, subject to emissions e_t, and implies an alternative trajectory for the carbon tax consistent with optimal budget exhaustion.

Importantly, both the SCC and carbon-budget rules suggest that deferring net-zero emissions beyond 2050 is optimal from a welfare perspective. This recommendation diverges from the Paris Agreement's fixed timeline and is rooted in the economic cost structure of abatement: eliminating the final units of emissions is disproportionately expensive. Therefore, an intertemporally optimal strategy involves postponing some abatement efforts, anticipating future declines in abatement costs. Although climate stabilization is still achieved by the end of the century, cumulative emissions remain equivalent to those under the baseline scenario.

7. Robustness analysis

In this final section, we conduct four additional exercises to test the robustness of our main findings. Specifically, we: *(i)* introduce sticky wages alongside sticky prices to capture broader nominal rigidities; *(ii)* modify the redistribution scheme for carbon tax revenues to evaluate alternative fiscal policies; *(iii)* incorporate capital accumulation into the production function to reflect investment dynamics; and *(iv)* model abatement as a durable good. These extensions leave the underlying drivers of greenflation and climateflation unchanged from our baseline analysis, as they do not alter the structural channels through which carbon taxes and climate damages exert pressure on marginal costs. However, they do affect the general equilibrium adjustment of the economy which in turn shapes how these inflationary forces materialize ex post.

7.1. **Sticky wages.** The inflation decomposition in subsection 4.3 reveals that real wages adjust rapidly in response to climate-induced damages. To examine whether wage rigidity amplifies the impact of climate shocks, particularly the phenomenon of greenflation, on realized inflation, we introduce nominal wage stickiness into the model. Specifically, we assume that: *(i)* the labor market exhibits monopolistic competition; *(ii)* households delegate wage-setting decisions to employment agencies, following the framework of Erceg et al. (2000); and *(iii)* there are quadratic adjustment costs associated with changes in individual nominal wages $W_{i,t}$ for $i \in [0, l_t]$:[29]

$$\mathcal{C}^w_{i,t} = \frac{\kappa_w}{2}\left(\frac{W_{i,t}}{W_{i,t-1}} - \pi^\star_t\right)^2 \frac{W_{i,t}}{P_t} n_{i,t}, \tag{31}$$

[29] Each household supplies a differentiated type of labor $n_{i,t}$ monopolistically. At each time t, a continuum of perfectly competitive "employment agencies" aggregates this specialized labor into a homogeneous labor input n^d_t, which is sold to firms according to the CES aggregator: $n^d_t = (\int_0^1 n_{i,t}^{(\zeta_w-1)/\zeta_w}\,\mathrm{d}i)^{\zeta_w/(\zeta_w-1)}$. Profit maximization by these agencies yields the labor demand for type-i labor as $n_{i,t} = (W_{i,t}/W_t)^{-\zeta_w} n^d_t$, where $W_t = \left(\int_0^1 W_{i,t}^{1-\zeta_w}, \mathrm{d}i\right)^{1/(1-\zeta_w)}$ is the aggregate nominal wage index. The parameter ζ_w denotes the elasticity of substitution between different labor types.

where $\kappa_w > 0$ denotes the wage stickiness parameter.

Figure 9 displays the trajectories of key macroeconomic variables under both the Paris Agreement scenario (top row) and the laissez-faire scenario (bottom row), for varying degrees of wage stickiness. In addition to the baseline case with flexible wages, we consider two alternative degrees of nominal wage rigidity: moderate rigidity with $\kappa_w = 10$ and pronounced rigidity with $\kappa_w = 20$. The results show that wage stickiness amplifies the inflationary response to climate shocks and leads to a more pronounced economic contraction. This occurs because slower real wage adjustment prevents households from fully absorbing the rise in firms' marginal costs associated with climate damages and carbon taxes. Consequently, the inflationary pressures from both climateflation and greenflation become more persistent, while the output gap widens. These findings are consistent with those of Olovsson and Vestin (2023) and Del Negro et al. (2023), who also report that nominal wage rigidity increases inflation during the energy transition in dynamic general equilibrium models.

FIGURE 9. The role of wage stickiness

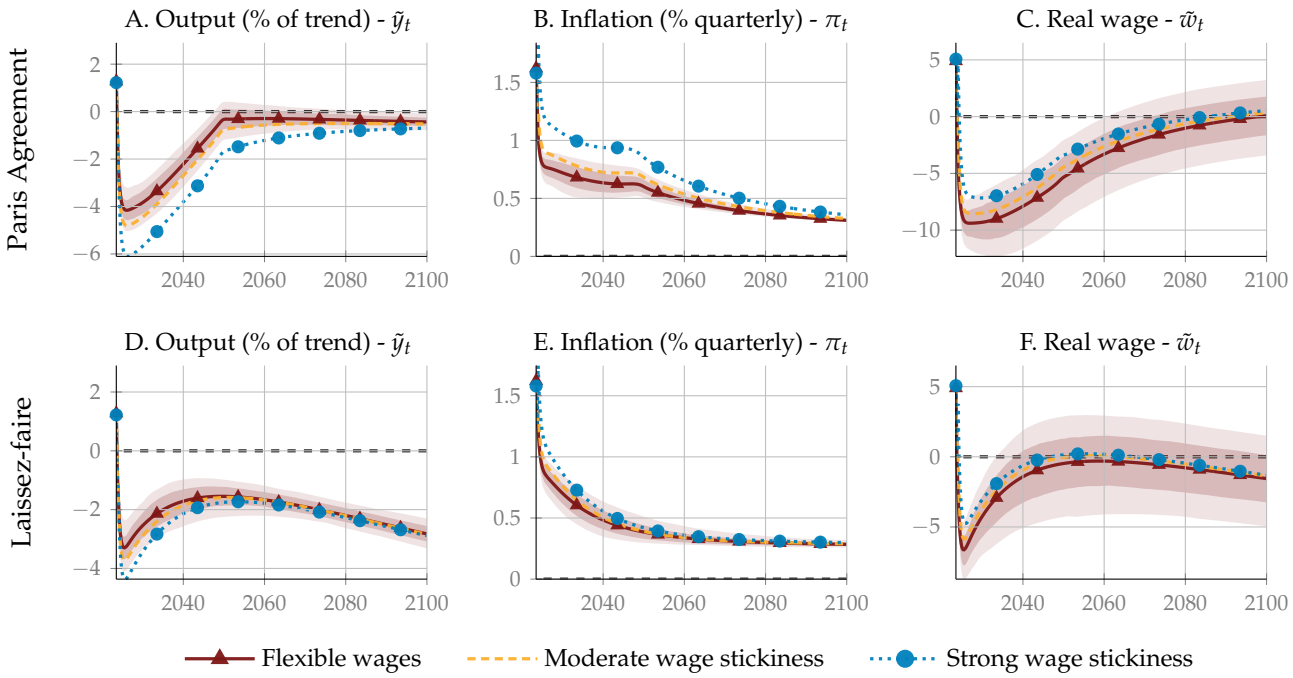

Note: The light red area denotes the uncertainty band under the flexible-wages assumption, based on 500 random draws generated using the Metropolis-Hastings sampler. The detrended real wage is defined as $\tilde{w}_t = w_t / z_t$.

7.2. **Redistribution of carbon tax revenues.** In the baseline scenario, carbon tax revenues are fully redistributed to Ricardian households for simplicity. In this setting, the transfers have a negligible effect on aggregate consumption, as Ricardian households are forward-looking and adjust their behavior primarily in response to changes in distorting taxes and interest

rates, not lump-sum transfers. However, alternative redistribution schemes can be explored by generalizing the transfer rule as:

$$d_{i,t} = z_t l_t \Phi\left(m_t\right) d + v \frac{T^e_{i,t}}{\omega}, \tag{32}$$

where $v \in [0,1]$ governs the share of carbon tax revenues redistributed to low-productivity households. The baseline case, denoted as "regressive redistribution", assumes $v = 0.$, meaning all transfers go to Ricardian households. Alternatively, a "flat transfer" scheme sets $v = 1/2$, under which both household types receive equal transfers. Finally, a "progressive redistribution" scheme is represented by $v = 2/3$, implying that low-productivity households receive twice as much as high-productivity households.

Figure 10 illustrates the macroeconomic effects of these three redistribution schemes under the Paris Agreement scenario. Increasing the share of carbon tax revenues allocated to low-productivity households leads to moderately higher aggregate output and consumption, thereby reducing the economic cost of the carbon tax. However, this redistribution also results in somewhat higher inflation, due to increased demand from more liquidity-constrained households. These findings are consistent with results from heterogeneous agent models such as Benmir and Roman (2022), Langot et al. (2023), and Auclert et al. (2023), which emphasize the importance of redistribution mechanisms in shaping the macroeconomic trajectory of green transitions. Our simpler two-type agent framework reinforces this insight, showing that even stylized redistribution rules can materially influence inflation dynamics.

FIGURE 10. The role of social transfers during the transition

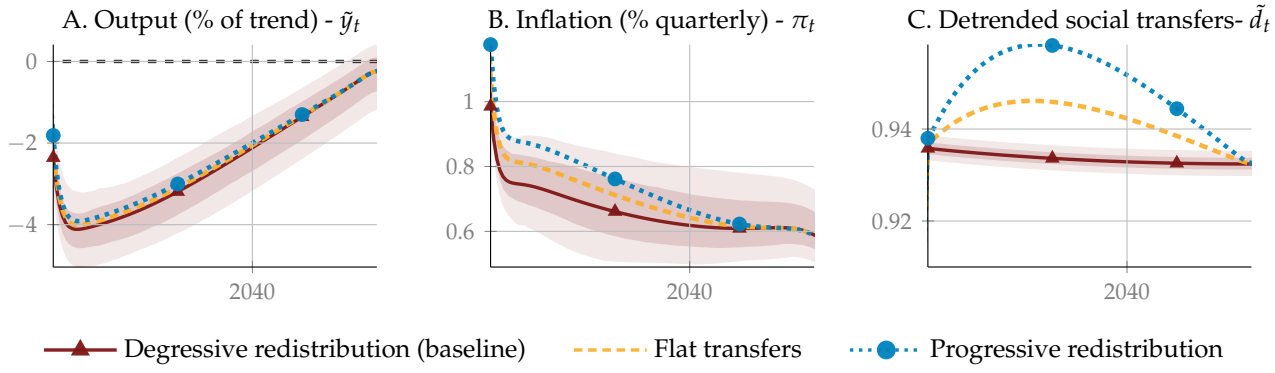

Note: The light red area denotes the uncertainty band under degressive redistribution (baseline) assumption, based on 500 random draws generated using the Metropolis-Hastings sampler.

7.3. **Capital in the production function.** Thus far, we have simplified the production side of the economy by considering labor as the sole input. This assumption facilitated the derivation of a tractable system of equations in the spirit of Woodford (2003). However, in integrated

assessment models such as DICE, capital plays a more prominent role in determining output and long-run growth. In this section, we explore whether and how the inclusion of capital affects the dynamics of the green transition.

To this end, we extend the production function of firm j to incorporate capital $k_{j,t}$ as follows:

$$y_{j,t} = \Phi(m_t) \left(z_t n_{j,t}^d \right)^{\alpha} k_{j,t-1}^{1-\alpha}. \tag{33}$$

The accumulation of capital is given by $k_{j,t} = (1-\delta)\, k_{j,t-1} + \left(1 - \mathcal{C}_{j,t}^{\iota}\right) \iota_{j,t}$, where δ is the capital depreciation rate, $\iota_{j,t}$ is investment and $\mathcal{C}_{j,t}^{\iota}$ are investment adjustment costs. These costs are given by $\mathcal{C}_{j,t}^{\iota} = \frac{\kappa_\iota}{2} \left(\frac{\iota_{j,t}}{\iota_{j,t-1}} - g_{z,t} \right)^2$, with κ_ι being a parameter that determines the magnitude of the costs.

FIGURE 11. The role of capital in the production function during the transition

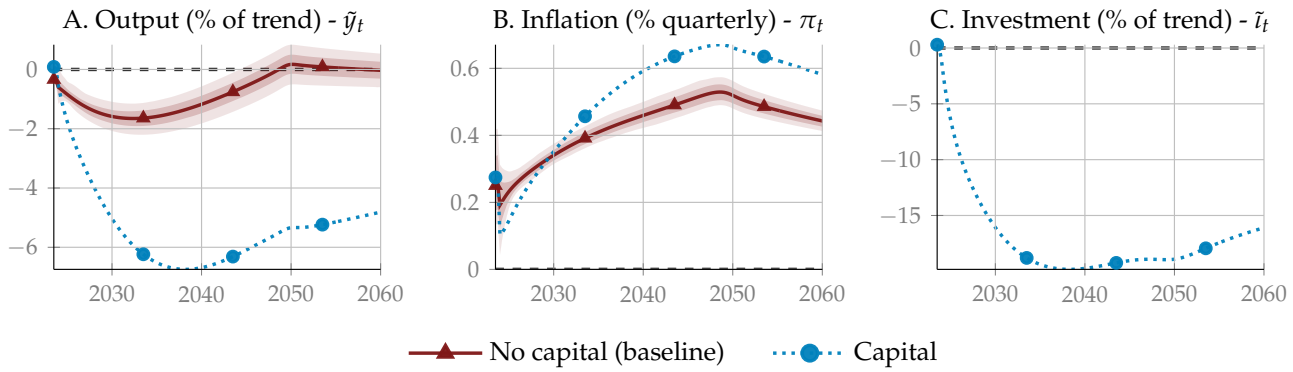

Note: The light red area denotes the uncertainty band under the no-capital (baseline) assumption, based on 500 random draws generated using the Metropolis-Hastings sampler. Detrended investment is defined as $\tilde{\iota}_t = \iota_t / (l_t z_t)$.

Figure 11 illustrates the trajectory of the economy under the Paris Agreement scenario, comparing outcomes with and without capital. In the extended model with capital, we set the depreciation rate to $\delta = 0.015$ and the investment adjustment cost parameter to $\kappa_\iota = 1$. The inclusion of capital reveals that the green transition leads to a pronounced crowding-out of conventional investment, which exacerbates the economic downturn and results in higher inflation. These effects highlight that introducing capital exacerbates our initial results, amplifying both the depth of the recession and the persistence of inflation during the green transition, thereby reinforcing the macroeconomic challenges associated with ambitious climate mitigation policies.

7.4. **Abatement as investment goods.** In standard DICE models, abatement is modeled as a flow variable that can adjust instantly and without cost in response to changes in the carbon tax. In reality, however, many abatement measures involve durable investments, such as

infrastructure, that are costly and not easily reversible. To reflect this, we modify Equation (9) to: $\mathcal{C}^a_{j,t} = \theta_{1,t}\Im^{\theta_2}_{j,t} y_{j,t}$, where $\Im_{j,t}$ denotes the flow of new durable abatement goods. The stock of abatement capital evolves according to $\mu_{j,t} = (1-\delta_\mu)\mu_{j,t-1} + \Im_{j,t}$, with $\delta_\mu = 0.025$, implying a 40-year average lifetime, consistent with infrastructure investment. In the DICE framework, cumulative abatement spending under the Paris Agreement scenario amount to 71% of 2020 GDP. We calibrate the cost parameter $\theta_{1,2020}$ up to 1,447 to match this benchmark.

Figure 12 illustrates the transition dynamics under the Paris Agreement scenario, comparing two assumptions about the lifetime of abatement goods. The red curve depicts the baseline case, where abatement goods are non-durable and expire after one period. In contrast, the blue dotted curve shows the scenario with durable abatement goods, where investments accumulate and persist over time. The results indicate that durability substantially increases the initial transition cost: achieving net-zero emissions requires large upfront investments with limited scope to defer expenditures. As a result, GDP declines by up to -5% in 2035, and inflationary pressures are nearly twice as high compared to the non-durable baseline.

FIGURE 12. Transition dynamics with durable abatement investments

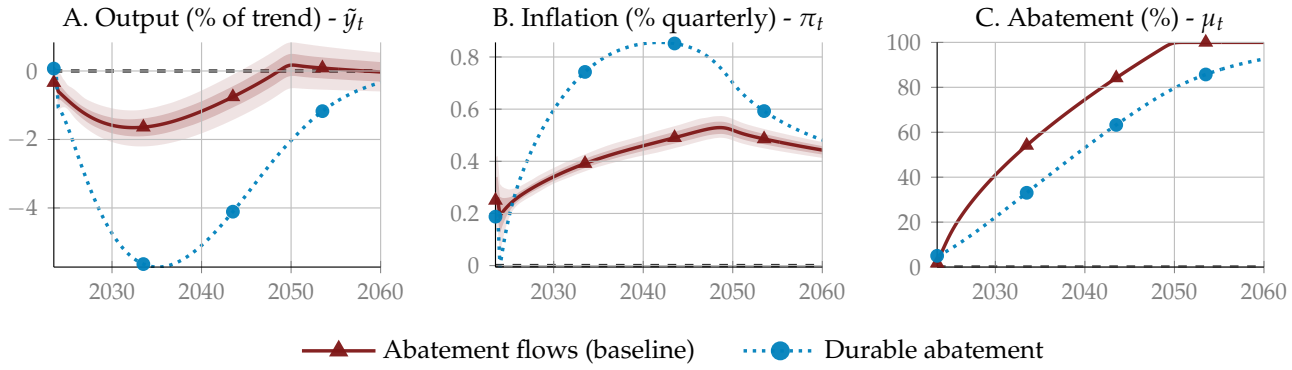

Note: The light red area denotes the uncertainty band under the abatement-flows (baseline) assumption, based on 500 random draws generated using the Metropolis-Hastings sampler.

8. CONCLUSION

This paper introduces the New Keynesian Climate (NKC) model, a unified macroeconomic framework that bridges the gap between long-term climate-economy dynamics and short- to medium-term monetary policy analysis. By extending the standard New Keynesian setup *à la* Woodford (2003) and Galí (2008) to include carbon stock accumulation, climate externalities, and abatement costs, the model provides a tractable and comprehensive tool for evaluating the real and nominal macroeconomic effects of climate interventions.

Our nonlinear, Bayesian-estimated model reveals that both climate change and mitigation efforts have significant implications for inflation, output, and interest rates, with nominal

rigidities playing a critical role. We find that Paris-aligned pathways to net-zero emissions generate higher and more persistent inflation than laissez-faire scenarios. In addition, monetary policy rules based on fixed steady-state interest rate tend to exacerbate these inflationary pressures. This highlights the need for central banks to adapt their frameworks to reflect a rising natural rate of interest and increased macroeconomic volatility during the green transition. Crucially, our results emphasize that carbon pricing must account for nominal frictions; otherwise, miscalibrated policies can lead to excessive inflation and reduced consumption, weakening public support for climate action.

Overall, effective climate policy cannot be decoupled from sound monetary policy. Ensuring both price stability and environmental sustainability demands that central banks evolve their strategies to meet the challenges of the green transition.

References

Adjemian, S. and Juillard, M. (2014). Assessing long run risk in a DSGE model under ZLB with the stochastic extended path approach. *Mimeo*, CEPREMAP.

Adjemian, S., Juillard, M., Karamé, F., Mutschler, W., Pfeifer, J., Ratto, M., Rion, N., and Villemot, S. (2024). Dynare: Reference manual, version 6. *Dynare Working Paper #80*, CEPREMAP.

Annicchiarico, B. and Di Dio, F. (2015). Environmental policy and macroeconomic dynamics in a New Keynesian model. *Journal of Environmental Economics and Management*, 69:1–21.

Auclert, A., Monnery, H., Rognlie, M., and Straub, L. (2023). Managing an energy shock: Fiscal and monetary policy. *Working Paper #31543*, National Bureau of Economic Research.

Auer, R., Borio, C., and Filardo, A. (2017). The globalisation of inflation: The growing importance of global value chains. *Working Paper #602*, Bank for International Settlements.

Bailey, M. J. (1956). The welfare cost of inflationary finance. *Journal of Political Economy*, 64:93–110.

Baleyte, J., Bazot, G., Monnet, E., and Morys, M. (2024). High temperature shocks are supply shocks. evidence from one century of monthly data. *Discussion Paper #19682*, Centre for Economic Policy Research.

Barrage, L. (2020). Optimal dynamic carbon taxes in a climate–economy model with distortionary fiscal policy. *The Review of Economic Studies*, 87:1–39.

Barrage, L. and Nordhaus, W. (2024). Policies, projections, and the social cost of carbon: Results from the dice-2023 model. *Proceedings of the National Academy of Sciences*, 121:e2312030121.

Benigno, P. and Eggertsson, G. B. (2023). It's baaack: The surge in inflation in the 2020s and the return of the non-linear Phillips curve. *Working Paper #31197*, National Bureau of Economic Research.

Benmir, G. and Roman, J. (2022). The distributional costs of net-zero: A hank perspective. *Mimeo*, London School of Economics.

Bilal, A. and Känzig, D. R. (2025). Does unilateral decarbonization pay for itself? *Working Paper #33364*, National Bureau of Economic Research.

Bilbiie, F., Ghironi, F., and Melitz, M. (2012). Endogenous entry, product variety, and business cycles. *Journal of Political Economy*, 120:304–345.

Cai, Y. and Lontzek, T. (2019). The social cost of carbon with economic and climate risks. *Journal of Political Economy*, 127:2684–2734.

Chow, G. C. and Lin, A.-L. (1971). Best linear unbiased interpolation, distribution, and extrapolation of time series by related series. *The Review of Economics and Statistics*, 53:372–375.

Christiano, L., Motto, R., and Rostagno, M. (2014). Risk shocks. *American Economic Review*, 104:27–65.

Clarida, R., Gali, J., and Gertler, M. (1999). The science of monetary policy: a new keynesian perspective. *Journal of Economic Literature*, 37:1661–1707.

Cochrane, J. H. (2001). Long-term debt and optimal policy in the fiscal theory of the price level. *Econometrica*, 69:69–116.

Coenen, G., Lozej, M., and Priftis, R. (2024). Macroeconomic effects of carbon transition policies: an assessment based on the ECB's new area-wide model with a disaggregated energy sector. *European Economic Review*, 167:104798.

Cuba-Borda, P., Guerrieri, L., Iacoviello, M., and Zhong, M. (2019). Likelihood evaluation of models with occasionally binding constraints. *Journal of Applied Econometrics*, 34:1073–1085.

Dechezleprêtre, A., Fabre, A., Kruse, T., Planterose, B., Sanchez Chico, A., and Stantcheva, S. (2025). Fighting climate change: International attitudes toward climate policies. *American Economic Review*, 115:1258–1300.

Del Negro, M., di Giovanni, J., and Dogra, K. (2023). Is the green transition inflationary? *Staff Reports #1053*, Federal Reserve Bank of New York.

Del Negro, M., Giannoni, M. P., and Patterson, C. (2023). The forward guidance puzzle. *Journal of Political Economy Macroeconomics*, 1:43–79.

Del Negro, M., Giannoni, M. P., and Schorfheide, F. (2015). Inflation in the great recession and new keynesian models. *American Economic Journal: Macroeconomics*, 7:168–196.

Di Tella, R., MacCulloch, R. J., and Oswald, A. J. (2001). Preferences over inflation and unemployment: Evidence from surveys of happiness. *American Economic Review*, 91:335–341.

Dietz, S., Van Der Ploeg, F., Rezai, A., and Venmans, F. (2021). Are economists getting climate dynamics right and does it matter? *Journal of the Association of Environmental and Resource Economists*, 8:895–921.

Erceg, C. J., Henderson, D. W., and Levin, A. T. (2000). Optimal monetary policy with staggered wage and price contracts. *Journal of Monetary Economics*, 46:281–313.

Fair, R. and Taylor, J. (1983). Solution and maximum likelihood estimation of dynamic nonlinear rational expectations models. *Econometrica*, 51:1169–1185.

Fernández-Villaverde, J., Gillingham, K., and Scheidegger, S. (2025). Climate change through the lens of macroeconomic modeling. *Annual Review of Economics*, Forthcoming.

Fernández-Villaverde, J., Rubio-Ramírez, J. F., and Schorfheide, F. (2016). Solution and estimation methods for DSGE models. In *Handbook of Macroeconomics*, volume 2, pages 527–724. Elsevier.

Fève, P., Matheron, J., and Sahuc, J.-G. (2010). Inflation target shocks and monetary policy inertia in the euro area. *The Economic Journal*, 120:1100–1124.

Finkelstein Shapiro, A. and Metcalf, G. E. (2023). The macroeconomic effects of a carbon tax to meet the US Paris Agreement target: The role of firm creation and technology adoption. *Journal of Public Economics*, 218:104800.

Folini, D., Friedl, A., Kübler, F., and Scheidegger, S. (2025). The climate in climate economics. *Review of Economic Studies*, 92:299–338.

Fornaro, L., Guerrieri, V., and Reichlin, L. (2025). Monetary policy for the green transition. *Mimeo*, Centre de Recerca en Economia Internacional.

Fried, S. (2022). Seawalls and stilts: A quantitative macro study of climate adaptation. *The Review of Economic Studies*, 89:3303–3344.

Galí, J. (2008). *Monetary policy, inflation, and the business cycle*. Princeton University Press.

Golosov, M., Hassler, J., Krusell, P., and Tsyvinski, A. (2014). Optimal taxes on fossil fuel in general equilibrium. *Econometrica*, 82:41–88.

Guerrieri, L. and Iacoviello, M. (2017). Collateral constraints and macroeconomic asymmetries. *Journal of Monetary Economics*, 90:28–49.

Harding, M., Lindé, J., and Trabandt, M. (2023). Understanding post-covid inflation dynamics. *Journal of Monetary Economics*, 140:S101–S118.

Hazell, J., Herreno, J., Nakamura, E., and Steinsson, J. (2022). The slope of the phillips curve: evidence from us states. *The Quarterly Journal of Economics*, 137:1299–1344.

Holston, K., Laubach, T., and Williams, J. C. (2017). Measuring the natural rate of interest: International trends and determinants. *Journal of International Economics*, 108:S59–S75.

IPCC (2021). Climate change 2021: The physical science basis.summary for policymakers. Contribution of Working Group I to the Sixth Assessment Report of the Intergovernmental Panel on Climate Change.

Ireland, P. N. (2007). Changes in the federal reserve's inflation target: Causes and consequences. *Journal of Money, Credit and Banking*, 39:1851–1882.

Jensen, S. and Traeger, C. P. (2014). Optimal climate change mitigation under long-term growth uncertainty: Stochastic integrated assessment and analytic findings. *European Economic Review*, 69:104–125.

Jo, A. and Miftakhova, A. (2024). How constant is constant elasticity of substitution? Endogenous substitution between clean and dirty energy. *Journal of Environmental Economics and Management*, 125:102982.

Jondeau, E., Levieuge, G., Sahuc, J.-G., and Vermandel, G. (2023). Environmental subsidies to mitigate net-zero transition costs. *Working Paper #910*, Banque de France.

Juillard, M. (1996). Dynare: A program for the resolution and simulation of dynamic models with forward variables through the use of a relaxation algorithm. *Working Paper #9602*, CEPREMAP.

Känzig, D. R. (2023). The unequal economic consequences of carbon pricing. *Working Paper #31221*, National Bureau of Economic Research.

Känzig, D. R. and Konradt, M. (2024). Climate policy and the economy: Evidence from europe's carbon pricing initiatives. *IMF Economic Review*, 72:1081–1124.

Langot, F., Malmberg, S., Tripier, F., and Hairault, J.-O. (2023). The macroeconomic and redistributive effects of shielding consumers from rising energy prices: A real time evaluation of the french experiment. *Working Paper #2305*, CEPREMAP.

Laubach, T. and Williams, J. C. (2003). Measuring the natural rate of interest. *Review of Economics and Statistics*, 85:1063–1070.

Leeper, E. M. (1991). Equilibria under 'active' and 'passive' monetary and fiscal policies. *Journal of Monetary Economics*, 27:129–147.

Lucas, Jr, R. E. (2000). Inflation and welfare. *Econometrica*, 68:247–274.

McKay, A., Nakamura, E., and Steinsson, J. (2017). The discounted Euler equation: A note. *Economica*, 84:820–831.

Nakov, A. and Thomas, C. (2023). Climate-conscious monetary policy. *Working Paper #2845*, European Central Bank.

Nordhaus, W. (1992). The 'DICE' model: Background and structure of a dynamic integrated climate-economy model of the economics of global warming. *Technical Report*, Cowles Foundation for Research in Economics, Yale University.

Nordhaus, W. D. (2017). Revisiting the social cost of carbon. *Proceedings of the National Academy of Sciences*, 114:1518–1523.

Nuño, G., Renner, P., and Scheidegger, S. (2024). Monetary policy with persistent supply shocks. *Working Paper #11463*, CESifo.

OECD (2017). Entrepreneurship at a Glance. *OECD Publishing*.

Olovsson, C. and Vestin, D. (2023). Greenflation? *Working Paper #420*, Sveriges Riksbank.

Orphanides, A. (2002). Monetary-policy rules and the great inflation. *American economic review*, 92:115–120.

Pappa, E., Airaudo, F., and Seoane, H. D. (2023). The green metamorphosis of a small open economy. *Discussion Paper #17863*, Centre for Economic Policy Research.

Pindyck, R. (2013). Climate Change Policy: What do the models tell us? *Journal of Economic Literature*, 51:860–872.

Rey, H. (2015). Dilemma not trilemma: The global financial cycle and monetary policy independence. *Working Paper #21162*, National Bureau of Economic Research.

Schnabel, I. (2022). A new age of energy inflation: climateflation, fossilflation and greenflation. In *Remarks at a panel on Monetary Policy and Climate Change at The ECB and its Watchers XXII Conference, Frankfurt am Main*, volume 17.

Shiller, R. J. (1997). Why do people dislike inflation? In *Reducing inflation: Motivation and strategy*, pages 13–70. University of Chicago Press.

Smets, F. and Wouters, R. (2007). Shocks and frictions in US business cycles: A Bayesian DSGE approach. *American Economic Review*, 97:586–606.

Van den Bremer, T. S. and Van der Ploeg, F. (2021). The risk-adjusted carbon price. *American Economic Review*, 111(9):2782–2810.

van der Ploeg, F. and Rezai, A. (2020). The risk of policy tipping and stranded carbon assets. *Journal of Environmental Economics and Management*, 100:102258.

Woodford, M. (1995). Price-level determinacy without control of a monetary aggregate. *Carnegie-Rochester Conference Series on Public Policy*, 43:1–46.

Woodford, M. (2003). *Interest and Prices: Foundations of a Theory of Monetary Policy*. Princeton University Press.

Online Appendix
–Not Intended for Publication–

APPENDIX A. FULL MODEL

This appendix presents the full set of equations. It includes four core equations and variables $\{\tilde{y}_t, \pi_t, r_t, m_t\}$:

$$\left(\frac{x_t\tilde{y}_t - \omega\tilde{d}_t}{1-\omega}\right)^{-\sigma_c} = \beta\mathbb{E}_t\left\{\frac{\varepsilon_{b,t+1}}{\varepsilon_{b,t}}\frac{r_t}{\pi_{t+1}}\left((1-\omega)\left(\frac{x_{t+1}\tilde{y}_{t+1} - \omega\tilde{d}_t}{1-\omega}\right)^{-\sigma_c} + \omega\tilde{d}_t^{\,-\sigma_c}\right)\right\} \tag{A.1}$$

$$(\pi_t - \pi_t^\star)\,\pi_t = (1-\vartheta)\beta\mathbb{E}_t\left\{(1+g_{z,t+1})\,\frac{\tilde{y}_{t+1}}{\tilde{y}_t}\,(\pi_{t+1} - \pi_{t+1}^\star)\,\pi_{t+1}\right\} + \frac{\zeta}{\kappa}\varepsilon_{p,t}mc_t + \frac{1-\zeta}{\kappa} \tag{A.2}$$

$$\frac{r_t}{r} = \left(\frac{r_{t-1}}{r}\right)^{\phi_r}\left[\left(\frac{\pi_t^\star}{\pi}\right)\left(\frac{\pi_t}{\pi_t^\star}\right)^{\phi_\pi}\left(\frac{\tilde{y}_t}{\tilde{y}_t^n}\right)^{\phi_y}\right]^{1-\phi_r}\varepsilon_t^r \tag{A.3}$$

$$m_t = m_{t-1} + \xi_m\sigma_t\left(1 - \tilde{\tau}_{e,t}^{\frac{1}{\theta_2-1}}\right)z_t l_t\tilde{y}_t\varepsilon_{e,t} \tag{A.4}$$

The model also includes auxiliary variables:

$$x_t = 1 - (1-\vartheta)\frac{\kappa}{2}(\pi_t - \pi_t^\star)^2 - \theta_{1,t}\tilde{\tau}_{e,t}^{\theta_2/(\theta_2-1)} - \vartheta(1-\epsilon_{p,t}mc_t) \tag{A.5}$$

$$mc_t = \frac{\psi}{\epsilon_{b,t}(1-\omega)^{\sigma_c+\sigma_n}}\frac{\left(x_t\tilde{y}_t - \omega\tilde{d}_t\right)^{\sigma_c}\tilde{y}_t^{\sigma_n}}{\Phi\,(m_t)^{1+\sigma_n}} + \theta_{1,t}\tilde{\tau}_{e,t}\left[\theta_2 + (1-\theta_2)\,\tilde{\tau}_{e,t}^{\frac{1}{\theta_2-1}}\right] \tag{A.6}$$

where $\tilde{y}_t = y_t/(z_t l_t y)$, $\tilde{d}_t = d_t/z_t$, $\tilde{\tau}_{e,t} = \tau_{e,t}\sigma_t\varepsilon_{e,t}/(\theta_2\theta_{1,t})$.

Finally, it comprises five trend related deterministic processes

$$\sigma_t = \sigma_{t-1}(1-g_{\sigma,t}) \quad \text{and} \quad g_{\sigma,t} = (1-\delta_\sigma)\,g_{\sigma,t-1}, \tag{A.7}$$

$$z_t = z_{t-1}(1+g_{z,t}) \quad \text{and} \quad g_{z,t} = (1-\delta_z)\,g_{z,t-1}, \tag{A.8}$$

$$\theta_{1,t} = (p_b/\theta_2)(1-\delta_{pb})^{t-t_0}\sigma_t, \tag{A.9}$$

$$l_t = l_{t-1}\,(l_\infty/l_{t-1})^{\ell_g}, \tag{A.10}$$

$$\pi_t^\star = \delta_{\pi^\star}\pi + (1-\delta_{\pi^\star})\pi_{t-1}^\star, \tag{A.11}$$

and four stochastic processes:

$$\varepsilon_{b,t} = (1-\rho_b) + \rho_b\varepsilon_{b,t-1} + \eta_{b,t}; \quad \varepsilon_{p,t} = (1-\rho_p) + \rho_p\varepsilon_{p,t-1} + \eta_{p,t};$$

$$\varepsilon_{e,t} = (1-\rho_e) + \rho_e\varepsilon_{e,t-1} + \eta_{e,t}; \quad \varepsilon_{r,t} = (1-\rho_r) + \rho_r\varepsilon_{r,t-1} + \eta_{r,t}.$$

APPENDIX B. THE EXTENDED PATH APPROACH

A perfect foresight algorithm typically requires *(i)* a finite number of periods and *(ii)* a terminal period to compute each endogenous variable in order to realize economic surprises. To fix notation, this general representation in the presence of extended path takes the form:

$$\tilde{y}_t = g_\Theta\left(y_0, y, 0\right) \tag{B.1}$$

$$y_t = \mathbb{E}_{t,t+S}\left\{g_\Theta\left(y_{t-1}, \tilde{y}_{t+S+1}, \varepsilon_t\right)\right\} \tag{B.2}$$

$$\mathcal{Y}_t = h_\Theta\left(y_t\right) \tag{B.3}$$

$$\varepsilon_t \sim \mathcal{N}\left(0, \Sigma_\varepsilon\right) \tag{B.4}$$

The first equation determines the deterministic evolution of the endogenous variables in the absence of shocks summarized in vector $\tilde{y}_t$ with initial conditions y_0 and terminal (asymptotic) state y for a given set of nonlinear equations $g_\Theta(\cdot)$. The second equation determines the path of endogenous variables y_t with economic surprise, ε_t is a vector of exogenous stochastic innovations that are normally distributed with mean zero and covariance Σ_ε; Θ is the vector of structural parameters; $h_\Theta(\cdot)$ and $g_\Theta(\cdot)$ are the set of nonlinear equations. $\mathbb{E}_{t,t+S}\{\cdot\}$ is the extended path-consistent expectation operator, which updates expectations over a specific time horizon of size S, and takes as given $\tilde{y}_{t+S+1}$ the terminal period of the expectation. Therefore, the size of the expectation window S must be sufficiently large to ensure that the value of $\tilde{y}_{t+S+1}$ does not affect the outcome.[30] The third equation relates the observations summarized in the vector $\mathcal{Y}_t$ to the endogenous variables in y_t. The last equation concerns the distribution of exogenous innovations.

For each evaluation of the sample likelihood, we first compute the deterministic path providing the transition between the initial period $\{\tilde{y}_t\}_{t=1}^{T}$ and the terminal period. We select a value of $T = 1{,}000$ to allow convergence to the terminal state. Formally, we use Equation B.1 assuming that (*i*) no shock with sequence $\{\varepsilon_t\}_{t=1}^{T}$ is all zeros, and (*ii*) a terminal condition that is the steady state of the model $\tilde{y}_{t+S+1} = y$, which can be written as $\tilde{y}_t = g_\Theta\left(y_{t_0}, y, 0\right)$. Next, we use the inversion filter to find the sequence of $\{\varepsilon_t\}_{t=1}^{T^*}$ that matches sample $\{\mathcal{Y}_t\}_{t=1}^{T^*}$ with T^* observations using $\{\tilde{y}_t\}_{t=1}^{T}$ as the terminal value of the expectation window. This implicitly assumes that agents expect the economy to return to its deterministic path $\tilde{y}$ after S periods. Based on the smoothed sequence $\{\varepsilon_t\}_{t=1}^{T^*}$, the likelihood function $\mathcal{L}(\theta, \mathcal{Y}_{1:T^*})$ of the model is obtained, conditional on the matrix of observations through time T^*.

[30] One must strike a balance between the length of the expectation window to mimic infinite-horizon rational expectations, and the computational burden of updating the expectations. We select an expectation horizon of 40 years ($S = 160$). This length is sufficiently large to ensure that the terminal conditions do not quantitatively affect the numerical value of the likelihood function, but exhibits a moderate computational burden.

APPENDIX C. OBSERVABLE VARIABLES

FIGURE C.1. Observable variables

APPENDIX D. MODEL EVALUATION

The model's empirical performance is first evaluated by comparing observed and model-implied moments, as reported in Table D.1. Data moments are computed over the period 1985Q1-2023Q2, while model-implied moments are derived from 1,000 random draws from the estimated posterior distributions of the model parameters. The table also includes 90% confidence intervals for the model-implied statistics. As shown in Table D.1, the model replicates key features of the data reasonably well, despite its relatively small scale.

TABLE D.1. Empirical and model-implied moments

	DATA	MODEL [5%;95%]	DATA	MODEL [5%;95%]
	Mean		**Standard deviations**	
Output growth	0.007	[0.007;0.008]	0.012	[0.011;.0.015]
Inflation rate	0.011	[0.000;0.016]	0.007	[0.005;0.012]
Nominal interest rate	0.008	[-0.001;0.017]	0.006	[0.004;0.013]
Carbon emission growth	0.004	[0.003;0.004]	0.013	[0.012;0.016]
	Autocorrelation		**Correlation w/ output**	
Output growth	-0.199	[-0.239;0.054]	1.000	[1.000;1.000]
Inflation rate	0.977	[0.835;0.976]	0.204	[-0.177;0.234]
Nominal interest rate	0.988	[0.967;0.996]	-0.038	[-0.175;0.236]
Carbon emission growth	-0.100	[-0.224;-0.064]	0.965	[0.877;0.945]

Note: Model-implied moments are computed across 1,000 random artificial series, each of the same size as the data sample.

Indeed, the model's performance is relatively strong when evaluated against typical benchmarks in the estimation of real business cycle models. In particular, it replicates the observed volatility of inflation and nominal interest rates with notable accuracy. However, the

model tends to underestimate the volatility of output and carbon emissions, indicating potential areas for refinement. First-order autocorrelations are generally well matched, although the persistence of inflation is somewhat understated relative to the data. In terms of cross-correlations with output, the model captures the key relationships for most variables, with the exception of carbon emission growth. This suggests that further calibration or structural enhancements may be necessary to better align the dynamics of carbon emissions with empirical observations.

As a second step, model performance is assessed using impulse response functions (IRFs), which provide insight into the dynamic propagation of shocks through the economic and climate systems. Figure D.1 presents the generalized impulse responses of the estimated model, based on parameters evaluated at their posterior mode from the Metropolis-Hastings sampling.

FIGURE D.1. Generalized impulse response functions of the estimated model

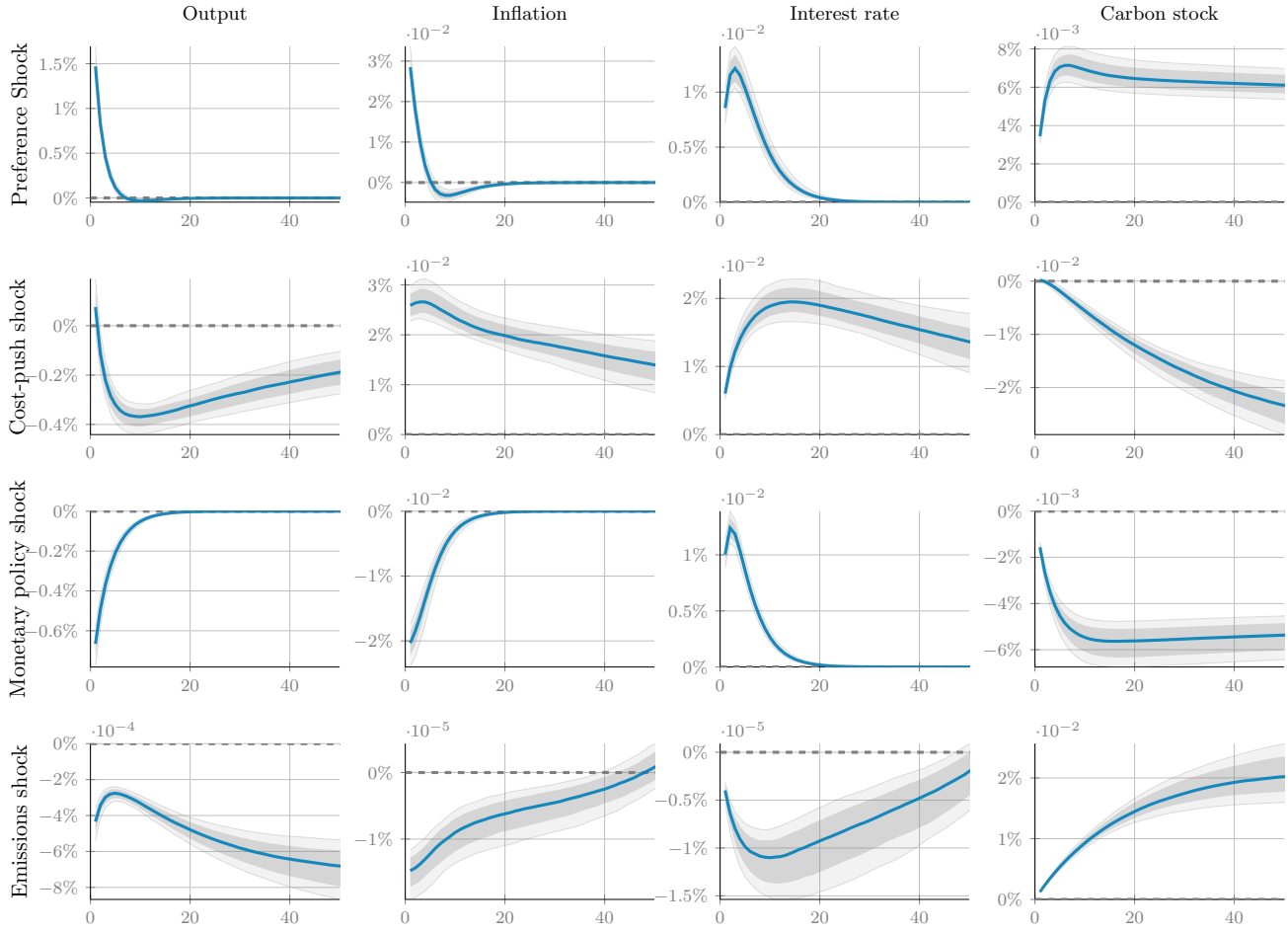

Note: The figure displays the generalized impulse response functions (GIRFs) of several variables for four shocks: preference, cost-push, monetary policy, and emissions in lines 1 to 4, respectively. The GIRFs are computed using the value of the state variables in 2023Q2, and each GIRF is expressed as a percentage deviation from its initial value in 2023. GIRFs are averaged based on 500 exogenous draws.

The first row of Figure D.1 presents the responses to a positive preference shock that raises household consumption. In response, aggregate output increases, reflecting the stimulative effect of heightened perceived wealth on economic activity. This boost in output, in turn, leads to a rise in both inflation and the cumulative carbon stock. To counteract the inflationary pressure from this demand-driven expansion, the central bank raises the nominal interest rate. As the shock dissipates over time, the tightening of monetary policy eventually induces a mild recession.

The second row of Figure D.1 reports the responses to a cost-push shock, similar to the markup shock in Smets and Wouters (2007). This adverse supply shock raises firms' pricing power and selling prices, exerting downward pressure on the rest of the economy. The central bank faces a classic trade-off between stabilizing prices and output, as the interest rate cannot simultaneously address movements in opposite directions. Following the shock, the real interest rate rises modestly, leading to a delayed contraction in output. Interestingly, the drop in economic activity has a beneficial environmental side effect: reduced emissions due to lower production and demand.

The third row of Figure D.1 illustrates the impact of a monetary policy shock, modeled as a temporary deviation of the nominal interest rate from the systematic component of the policy rule. This shock increases the return on safe assets, discouraging consumption and compressing aggregate demand. Firms respond by cutting labor demand, which reduces equilibrium wages and marginal costs. Consequently, both output and prices decline, leading to a reduction in emissions and a lower-than-expected carbon stock.

The fourth row shows the effects of an emission intensity shock, interpreted as an exogenous increase in emissions per unit of output. This shock raises the carbon stock in the atmosphere and imposes moderate economic damage. However, its effects on inflation and nominal interest rates are negligible, suggesting that such shocks may have limited short-run macroeconomic implications.

Finally, Figure D.2 presents a historical decomposition of output, inflation, and the nominal interest rate, attributing their fluctuations to the identified structural shocks within the New Keynesian climate model. This decomposition offers a dynamic interpretation of the drivers behind key macroeconomic variables over time.

FIGURE D.2. Historical decomposition of detrended output, inflation and the nominal interest rate over the sample period

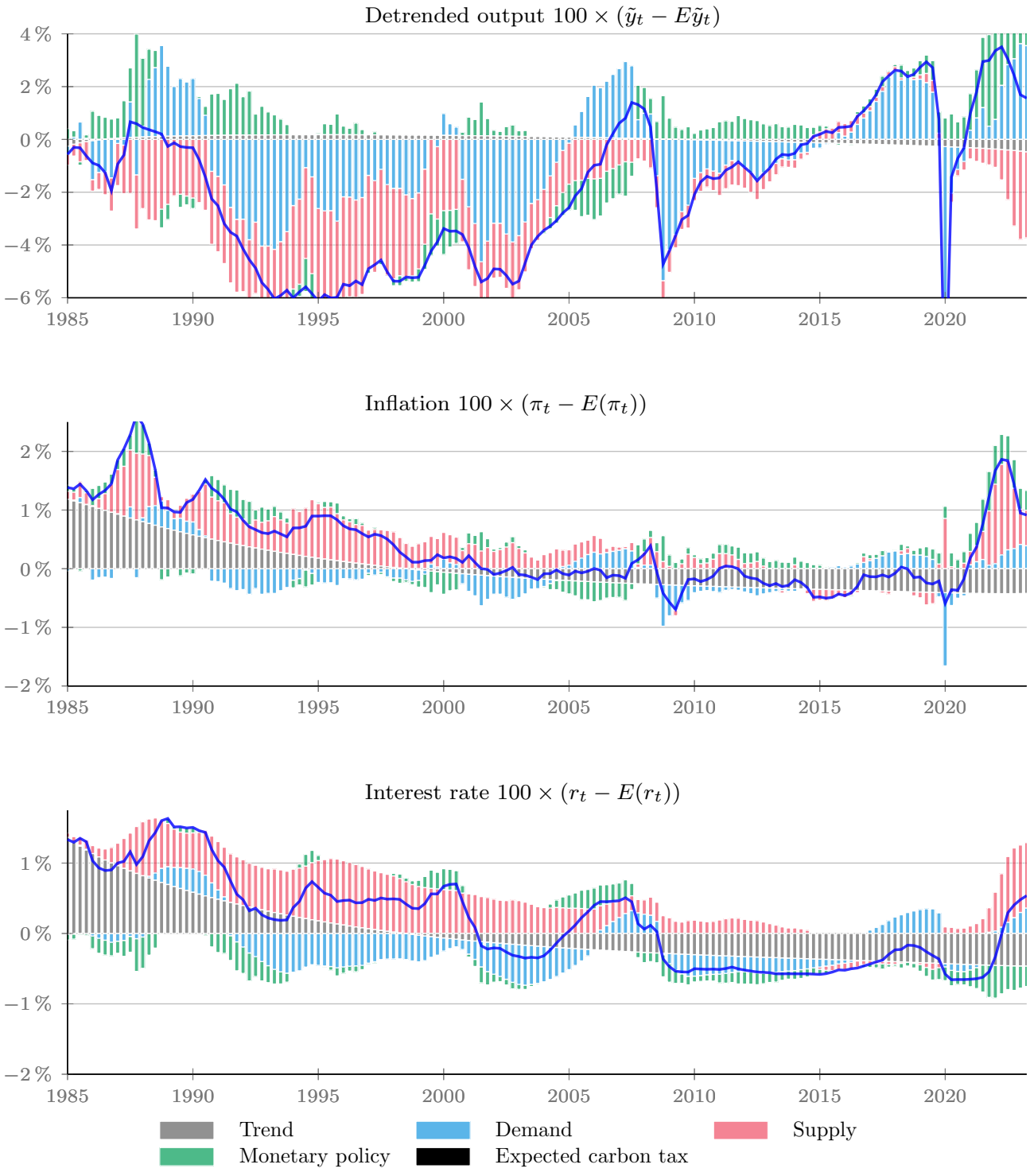

Note: This figure illustrates the approximate contribution of each structural shock to the determination of the variable of interest. Cross-products between shock contributions are omitted in the decomposition.

APPENDIX E. MATH DERIVATIONS

This appendix provides additional details on the decomposition of output and inflation.

E.1. **Demand part.** Detrended Euler equation reads as:

$$\tilde{\lambda}_t = \mathbb{E}_t \left\{ \beta \frac{r_t}{\pi_{t+1}} \left((1-\omega)\tilde{\lambda}_{t+1} + \omega \varepsilon_{b,t+1} \tilde{d}_t^{-\sigma_c} \right) \right\}. \tag{E.1}$$

It can be rewritten as:

$$\begin{aligned} \tilde{\lambda}_t &= \mathbb{E}_t \left\{ R_t \left((1-\omega)\tilde{\lambda}_{t+1} + \omega \varepsilon_{b,t+1} \tilde{d}_t^{-\sigma_c} \right) \right\} \\ &= \omega \mathbb{E}_t \left\{ \sum_{s=0}^{\infty} (1-\omega)^s \varepsilon_{b,t+s} \tilde{d}_{t+s}^{-\sigma_c} \prod_{j=0}^{s} R_{t+j} \right\}, \end{aligned}$$

where $R_t = \beta r_t / \pi_{t+1}$.

Recall that: $\tilde{\lambda}_t = \varepsilon_{b,t} \left(\frac{\tilde{c}_t - \omega \tilde{d}_t}{1-\omega} \right)^{-\sigma_c}$, the Euler equation becomes:

$$\left(\frac{c_t/z_t - \omega \tilde{d}_t}{(1-\omega)} \right)^{-\sigma_c} = \omega \mathbb{E}_t \left\{ \sum_{s=0}^{\infty} (1-\omega)^s \varepsilon_{b,t+s} \tilde{d}_{t+s}^{-\sigma_c} \prod_{j=0}^{s} R_{t+j} \right\}$$

which can be rewritten as:

$$c_t/z_t = IS_t,$$

where $IS_t = \omega \tilde{d}_t + (1-\omega) \left[\omega \mathbb{E}_t \left\{ \sum_{s=0}^{\infty} \beta (1-\omega)^s \varepsilon_{b,t+s} \tilde{d}_{t+s}^{-\sigma_c} \prod_{j=0}^{s} \frac{r_{t+j}}{\pi_{t+1+j}} \right\} \right]^{-1/\sigma_c}$.

In addition, we know that:

$$IS_t = c_t/z_t = x_t y_t/(z_t l_t),$$

where $x_t = 1 - (1-\vartheta)\frac{\kappa}{2} (\pi_t - \pi_t^\star)^2 - \theta_{1,t} \tilde{\tau}_{e,t}^{\theta_2/(\theta_2-1)} - \vartheta(1 - \epsilon_{p,t} mc_t)$, with $\mu_t = \tilde{\tau}_{e,t}^{1/(\theta_2-1)}$.

As $c_t = x_t y_t / l_t$, it comes:

$$IS_t = x_t \tilde{y}_t.$$

Therefore, applying the logarithm yields:

$$\hat{y}_t \simeq \widehat{IS}_t + \theta_{1,t} \tilde{\tau}_{e,t}^{\theta_2/(\theta_2-1)} + (1-\vartheta)\frac{\kappa}{2} (\pi_t - \pi_t^*)^2 + \vartheta(1 - \epsilon_{p,t} mc_t),$$

with $\hat{y}_t = \log(\tilde{y}_t/\tilde{y})$ and $\widehat{IS}_t = \log(IS_t/IS)$.

E.2. **Supply part.** The marginal cost is given by:

$$mc_t = \frac{w_t}{\Gamma_t} + \theta_{1,t} \mu_t^{\theta_2} + \tau_{e,t} \sigma_t (1-\mu_t) \varepsilon_{e,t}$$

Let us consider the real wage of the high productive worker $w_t = \psi_t n_t^{\sigma_n}/\lambda_t$, the general equilibrium condition $(1-\omega) n_t = n_t^d = N_t$ and the production function $y_t = l_t \Gamma_t N_t^\alpha$, we

obtain:

$$mc_t = \frac{1}{\lambda_t \Gamma_t} \psi_t \left(\left(\frac{y_t}{l_t \Gamma_t} \right)^{\frac{1}{\alpha}} \frac{1}{1-\omega} \right)^{\sigma_n} + \theta_{1,t} \mu_t^{\theta_2} + \tau_{e,t} \sigma_t \left(1 - \mu_t\right) \varepsilon_{e,t}$$

Recall that $\Gamma_t = \Phi\left(m_t\right) z_t$ and $\tilde{y}_t = y_t / \left(l_t z_t\right)$, thus:

$$mc_t = \frac{1}{\lambda_t \Phi\left(m_t\right)} \psi z_t^{-\sigma_c} \left(\left(\frac{\tilde{y}_t}{\Phi\left(m_t\right)} \right)^{\frac{1}{\alpha}} \frac{1}{1-\omega} \right)^{\sigma_n} + \theta_{1,t} \mu_t^{\theta_2} + \tau_{e,t} \sigma_t \left(1 - \mu_t\right) \varepsilon_{e,t}$$

Next, replacing λ_t by its expression in function of $\tilde{c}_t$ gives:

$$mc_t = \frac{\psi}{\varepsilon_{b,t} \left(\frac{\tilde{c}_t - \omega \tilde{d}_t}{1-\omega} \right)^{-\sigma_c} \Phi\left(m_t\right)} \left(\left(\frac{\tilde{y}_t}{\Phi\left(m_t\right)} \right)^{\frac{1}{\alpha}} \frac{1}{1-\omega} \right)^{\sigma_n} + \tilde{\tau}_{e,t} \theta_{1,t} \left(\theta_2 + \tilde{\tau}_{e,t}^{\frac{1}{\theta_2 - 1}} \left(1 - \theta_2\right) \right).$$

Finally,

$$mc_t = \frac{\psi}{\left(1-\omega\right)^{\sigma_c + \sigma_n}} \frac{\left(x_t \tilde{y}_t - \omega \tilde{d}_t\right)^{\sigma_c} \tilde{y}_t^{\frac{\sigma_n}{\alpha}}}{\varepsilon_{b,t} \Phi\left(m_t\right)^{1 + \frac{\sigma_n}{\alpha}}} + \tilde{\tau}_{e,t} \theta_{1,t} \left(\theta_2 + \tilde{\tau}_{e,t}^{\frac{1}{\theta_2 - 1}} \left(1 - \theta_2\right) \right).$$

Consequently, the Phillips curve is simply the discounted sum of future marginal costs:

$$\pi_t = \frac{\zeta}{\kappa} \mathbb{E}_t \sum_{s=0}^{\infty} \hat{\beta}_{t,t+s} \left[\varepsilon_{p,t+s} mc_{t+s} + \frac{1-\zeta}{\zeta} \right],$$

with $\hat{\beta}_{t,t+s} = [\beta(1-\vartheta)]^s \frac{y_{t+s} l_t}{y_t l_{t+s}} \frac{1}{\pi_t - \pi_t^\star}$.

Appendix F. Sensitivity analysis

This appendix presents a sensitivity analysis exploring the impact of various structural parameters on inflation and output dynamics during the green transition.

F.1. **The role of attenuated expectations.** The forward guidance puzzle in New Keynesian models underscores a well-known issue: these models often predict unrealistically large effects of future policy announcements on current economic outcomes, leading to implausibly strong responses in output and inflation. A similar dynamic arises with an announced carbon tax, which induces disproportionately large anticipatory adjustments in current consumption and investment, driven by expectations of future policy impacts. To address this concern, we examine the sensitivity of our model to this puzzle. Our framework incorporates two key parameters, one in the Euler equation and another in the Phillips curve, that moderate the influence of forward-looking real interest rates and marginal costs on present economic dynamics. Panel A of Figure F.1 illustrates the average levels of inflation, output, nominal interest rate, and real interest rate under varying degrees of attenuation. Stronger attenuation, implemented through more intense discounting of future marginal utilities of consumption,

tends to increase inflation. By assigning less weight to future real interest rates, households front-load consumption during the transition, creating upward pressure on prices through the demand channel.

FIGURE F.1. Sensitivity to structural parameters

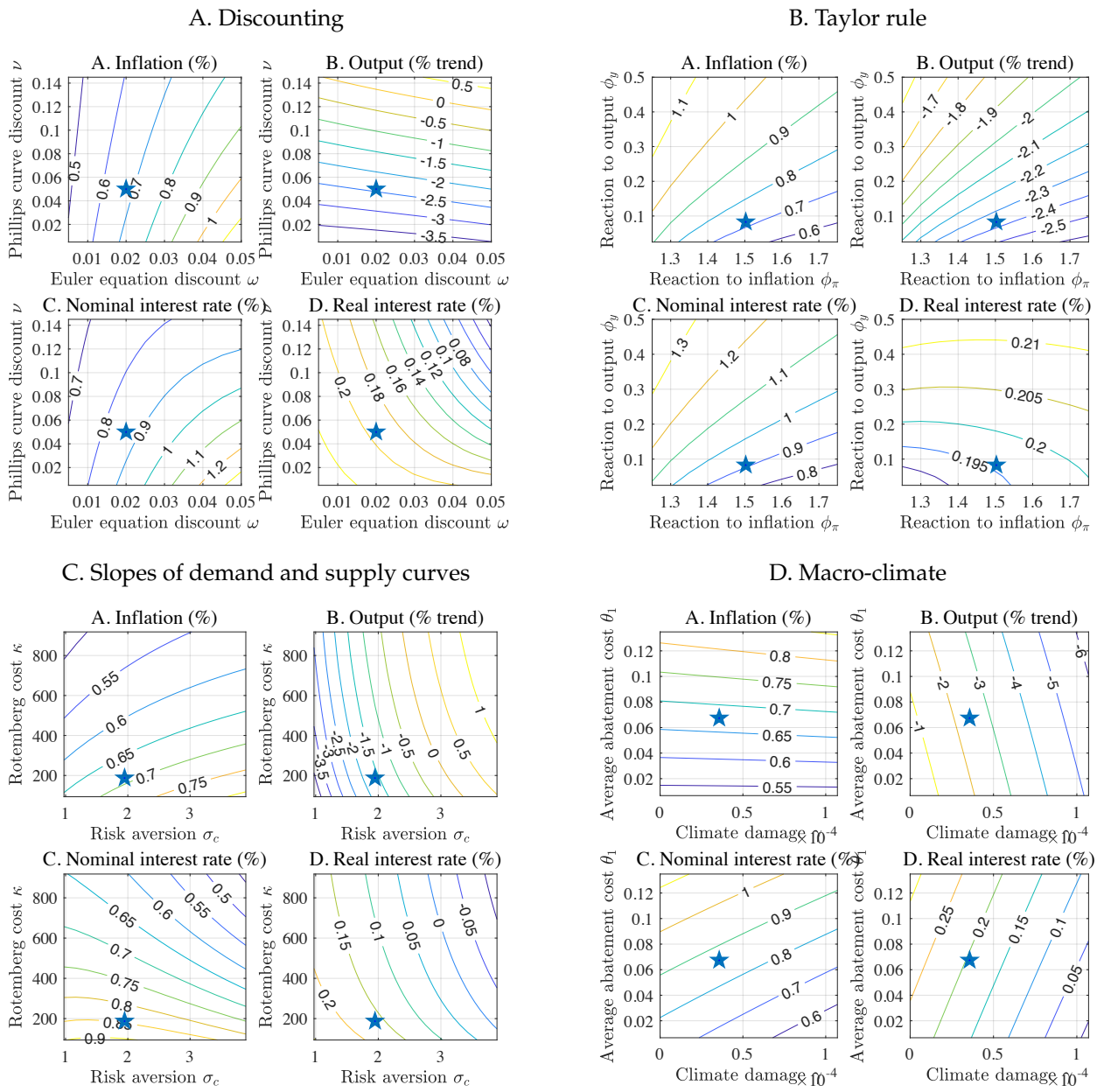

Note: This figure presents the average values of inflation, output, nominal interest rate, and real interest rate over the period from 2023Q4 to 2050Q1 under the Paris Agreement scenario. The star marker indicates the outcome based on the estimated parameter values.

Conversely, increased discounting also weakens the responsiveness of inflation to anticipated future marginal costs, such as those induced by a rising carbon tax, by flattening the

Phillips curve. This dampens inflationary pressures, and as a result, the economy experiences higher average output during the transition period due to more stable price dynamics.

F.2. **The Taylor rule.** An additional question concerns whether the monetary policy stance, characterized as either dovish or hawkish, influences macroeconomic dynamics during the transition period. To assess this, we vary the coefficients of the Taylor rule, focusing on a relatively high responsiveness to inflation $\phi_\pi \in [1.15, 2]$ and output $\phi_y \in [0.1, 1]$. Panel B of Figure F.1 presents the resulting outcome. Our findings are consistent with standard monetary stabilization mechanisms: increasing the inflation (respectively, output gap) coefficient tends to reduce average inflation (respectively, detrended output) during the transition. However, these effects are modest. A higher policy response coefficient does not lead to a proportionally large decline in the average value of the corresponding target variable. This result implies that the typical output-inflation trade-off, as discussed in Clarida et al. (1999) and Woodford (2003), is relatively weak in the context of the green transition. Furthermore, our analysis reveals that the divine coincidence, the principle whereby stabilizing inflation inherently stabilizes the output gap, does not hold. Specifically, increasing the weight on the output gap in the Taylor rule does not lead to a reduction in inflation. This suggests that the transition exhibits features of a supply-side shock, wherein attempts to stabilize real activity may be less effective in simultaneously managing price stability.

F.3. **Slopes of aggregate demand and supply curves.** Recent literature, including Hazell et al. (2022), has documented the relative flatness of the New Keynesian Phillips Curve (NKPC) since the 1980s. However, the recent surge in inflation, particularly following the economic disruptions caused by the war in Ukraine, has prompted a substantial reassessment of the price-setting mechanism. This reassessment has resulted in a significantly steeper NKPC, as shown in studies such as Harding et al. (2023) and Benigno and Eggertsson (2023). In light of these developments, we examine the sensitivity of our results to changes in the slope of the Phillips curve by varying the Rotemberg adjustment cost parameter from 50 to 120. In parallel, we also investigate the impact of the risk aversion coefficient in the household utility function. Within the New Keynesian framework, higher risk aversion reduces the responsiveness of households to real interest rate fluctuations, thereby weakening the monetary policy transmission channel. To this end, we explore values starting from 1.4, as used in Smets and Wouters (2007) and Nordhaus (2017), up to levels more commonly employed in the asset pricing literature. Panel C of Figure F.1 presents the outcomes of these sensitivity exercises. We find that increasing the degree of nominal rigidity does reduce the responsiveness of inflation during the transition; however, the effect is quantitatively limited and

does not materially alter the qualitative behavior of the model. This indicates that inflation dynamics during the transition are not highly sensitive to the specific calibration of nominal rigidities. By contrast, the risk aversion parameter plays a more critical role in shaping macroeconomic outcomes. A higher degree of risk aversion amplifies households' preference for consumption smoothing, reducing their sensitivity to real interest rate changes. As a result, aggregate consumption becomes less reactive to monetary policy shocks. This mechanism is especially important in determining output dynamics during the transition: when output is less sensitive to the real interest rate, contractionary effects from monetary tightening are mitigated. Under such conditions, abatement expenditures can become the dominant force, potentially allowing for an expansionary path even in the presence of carbon pricing and structural transformation.

F.4. **Macro-climate parameters.** We also examine the sensitivity of key macroeconomic variables to changes in macro-climate parameters. Specifically, Panel D of Figure F.1 presents the outcomes associated with varying the climate damage parameter (γ) and the abatement cost parameter (θ_1). To interpret γ, consider that in the baseline scenario with no mitigation policy, a carbon stock of 1,700 gigatons results in a total factor productivity loss of approximately 6.83%. We explore a range of values for γ, from zero climate damages to three times the calibrated baseline level (approximately 1.1×10^{-4}). For the abatement cost parameter θ_1, this can be interpreted as the average share of GDP required to achieve net-zero emissions. In our benchmark scenario, this cost is about 6.5% of GDP; we extend the analysis up to 13% of GDP to reflect more challenging decarbonization pathways. Our results indicate that inflation increases with both higher climate damages and higher abatement costs. This pattern is consistent with the earlier discussion of greenflation and climateflation. The imposition of carbon pricing policies, coupled with climate-induced disruptions to productivity, exerts upward pressure on production costs, thereby fueling inflation. Among the two parameters, abatement costs play a relatively larger role in shaping the cost of the transition. Higher abatement costs increase firms' marginal production costs, intensifying inflationary pressures through the greenflation channel. Similarly, a higher damage parameter raises inflation through the climateflation mechanism, while also exerting a contractionary effect on output. As damages grow, productivity deteriorates and real interest rates rise, which in turn reduces investment and consumption. Thus, the damage parameter emerges as a key driver of output dynamics during the transition period.